Report No. HA-38

Centre for Radio Science

A STUDY OF MEASUREMENT AND ANALYSIS OF MICROWAVE PROPAGATION CONDITIONS ACROSS THE BAY OF FUNDY

W.I. Lam and A.R. Webster

Final Report

DSS Contract No.
03SU.36001-1-1054

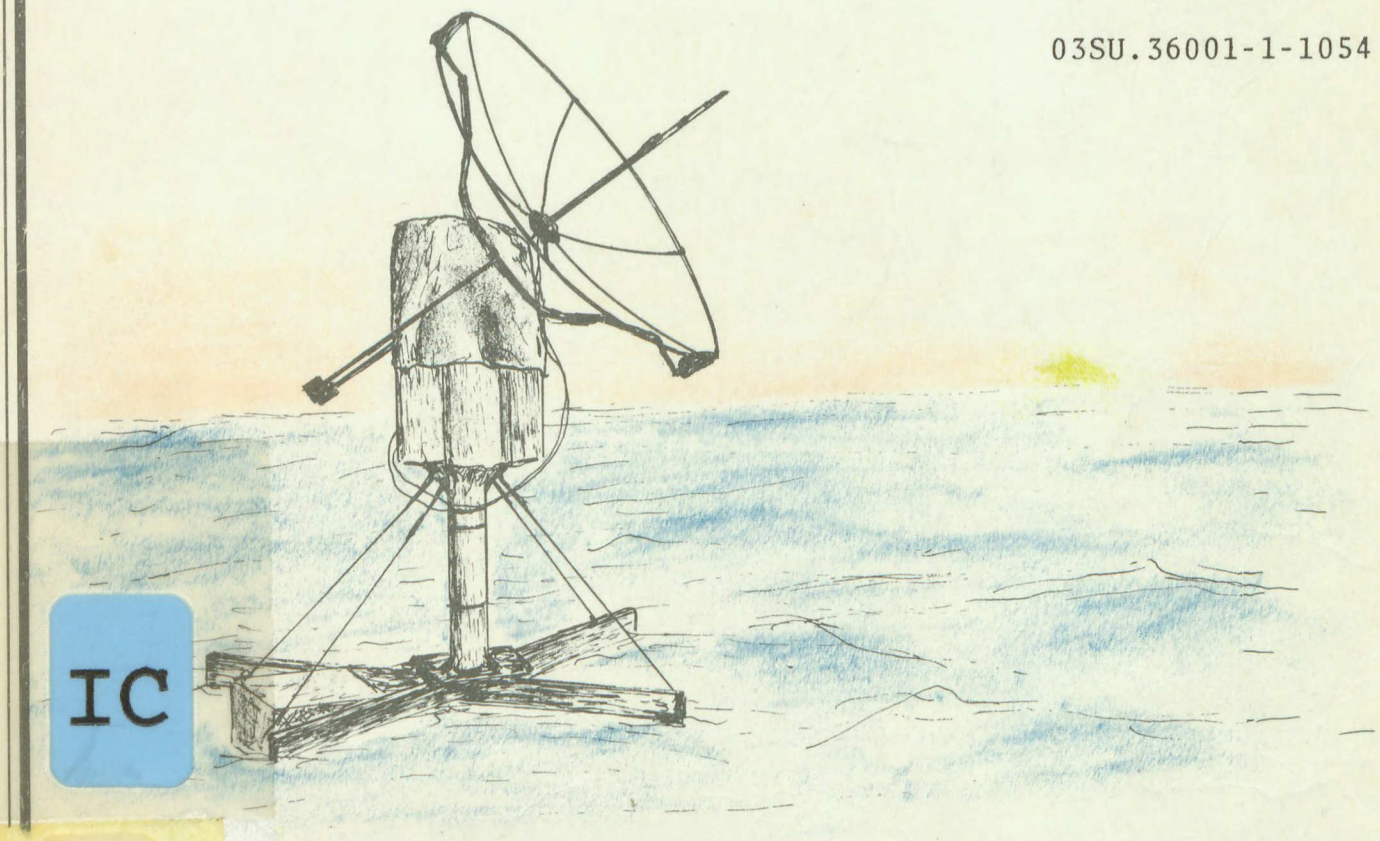

THE UNIVERSITY OF WESTERN ONTARIO
LONDON CANADA N6A 3K7

July, 1982

A STUDY OF MEASUREMENT AND ANALYSIS OF MICROWAVE PROPAGATION CONDITIONS ACROSS THE BAY OF FUNDY

A Final Report under

Department of Supplies and Services

Contract No. 03SU.36001-1-1054

Submitted to

Communications Research Centre

Department of Communications, Canada

by

Centre for Radio Science

University of Western Ontario

London, Canada

Principal Investigator: A.R. Webster

Research Associate: W.I. Lam

Report prepared by: W.I. Lam

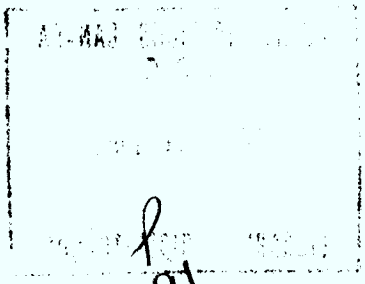

ABSTRACT

A microwave propagation experiment was performed on a line-of-sight path across the Bay of Fundy during the summer of 1981. The Microwave Diagnostic System employed in the experiment was configured to measure various ray path parameters including the number of ray paths, the amplitude and angle-of-arrival of the individual ray path(s), and the relative delay between rays. A digital radio test was carried out simultaneously on the same propagation path by the Maritime Tel. and Tel. and the New Brunswick Tel. using a Northern Telecom RD-3 Digital Radio. Results from the propagation experiment are presented and, where appropriate, correlated with results from the digital radio experiment.

TABLE OF CONTENTS

LIST OF FIGURES

1. INTRODUCTION

A microwave propagation experiment was performed on a path across the Bay of Fundy during the summer of 1981. The 80 km path from Otter Lake, N.B., to Nictaux South, N.S., constitutes one of the proposed communications links across the Bay of Fundy as a part of the Trans-Canada Telephone System. The experiment was an extension of a previous test that was performed across the Bay of Fundy from Otter Lake, N.B., to Aylesford, N.S. during the summer of 1980.

The experimental equipment used was a sweep-frequency phase-swept interferometer that employed a sweep in frequency from 9.505 to 10.513 GHz. The parameters that may be determined from the experimental measurements include the amplitude, the angle-of-arrival, and the relative path delays of the individual received ray path(s) under normal or multipath conditions.

In addition to the propagation experiment, a Northern Telecom RD-3 Digital Radio was operated by Maritime Tel. and Tel. and New Brunswick Tel. on the same propagation path during the same time period. Data regarding the performance of the digital radio during various time periods was kindly provided by the above companies and this provides further insight into the nature of propagation-induced impairments suffered by digital radio systems.

Up to the present time, much effort has been spent on the analysis of the data obtained from the propagation

experiment with emphasis on the time periods when outages were observed on the digital radio. So far, certain interesting observations have already emerged. However, due to the enormous amounts of data available, much remains to be done and continuing efforts should prove to be fruitful to the understanding of propagation anomalies and their effects on digital radio systems.

2. EXPERIMENTAL DETAILS

The Microwave Diagnostic System was shipped out to experimental sites in mid-July, 1981. After initial equipment set-up and antenna installation, the Diagnostic System, together with the Digital Radio System, was operated virtually uninterrupted from 31st July to 3rd September through the active fading month of August.

2.1 The Microwave Diagnostic System

The microwave diagnostic system used in the propagation experiment was developed at the University of Western Ontario through contracts with the Communications Research Centre of the Department of Communications. The principle of operation and equipment details were described in previous reports (Webster, 1977).

Briefly, the receiver was a 2-antenna interferometer receiver system. The receiving antennas were arranged vertically and spaced 3 metres apart. The transmitter transmitted a CW signal that was swept in frequency through a

1 GHz band (9.505 to 10.513 GHz) every 10 seconds. The sweep had a duration of 1.28 sec and was done via 64 frequency steps each spaced 16 MHz apart. The receiver local oscillator was synchronized to the received signal and, at each frequency step, the received amplitude on one of the antennas and the relative phase between the signals received on the two antennas were measured and recorded. From the sweep data, various properties of the received signal may be determined. These properties include the number of received ray paths, the relative amplitude, the angle-of-arrival, and the relative delay associated with the individual received rays. A summary of the Diagnostic System parameters is given in Appendix A.

In an effort to further improve on the reliability of the Diagnostic System in field operations, modifications were performed on the power supply and phase-locking sections of the receiver prior to its operation in the Bay of Fundy. The complete block diagram of the receiver is shown in Figure 2-1.

The transmit and receive antennas were mounted on telephone company towers at heights of 69 m and 81 m above ground respectively. Furthermore, the transmit antennas were mounted slightly below the digital radio antenna while the receive antenna was mounted above the digital radio antennas. The arrangement effectively provided almost identical propagation paths for the two tests.

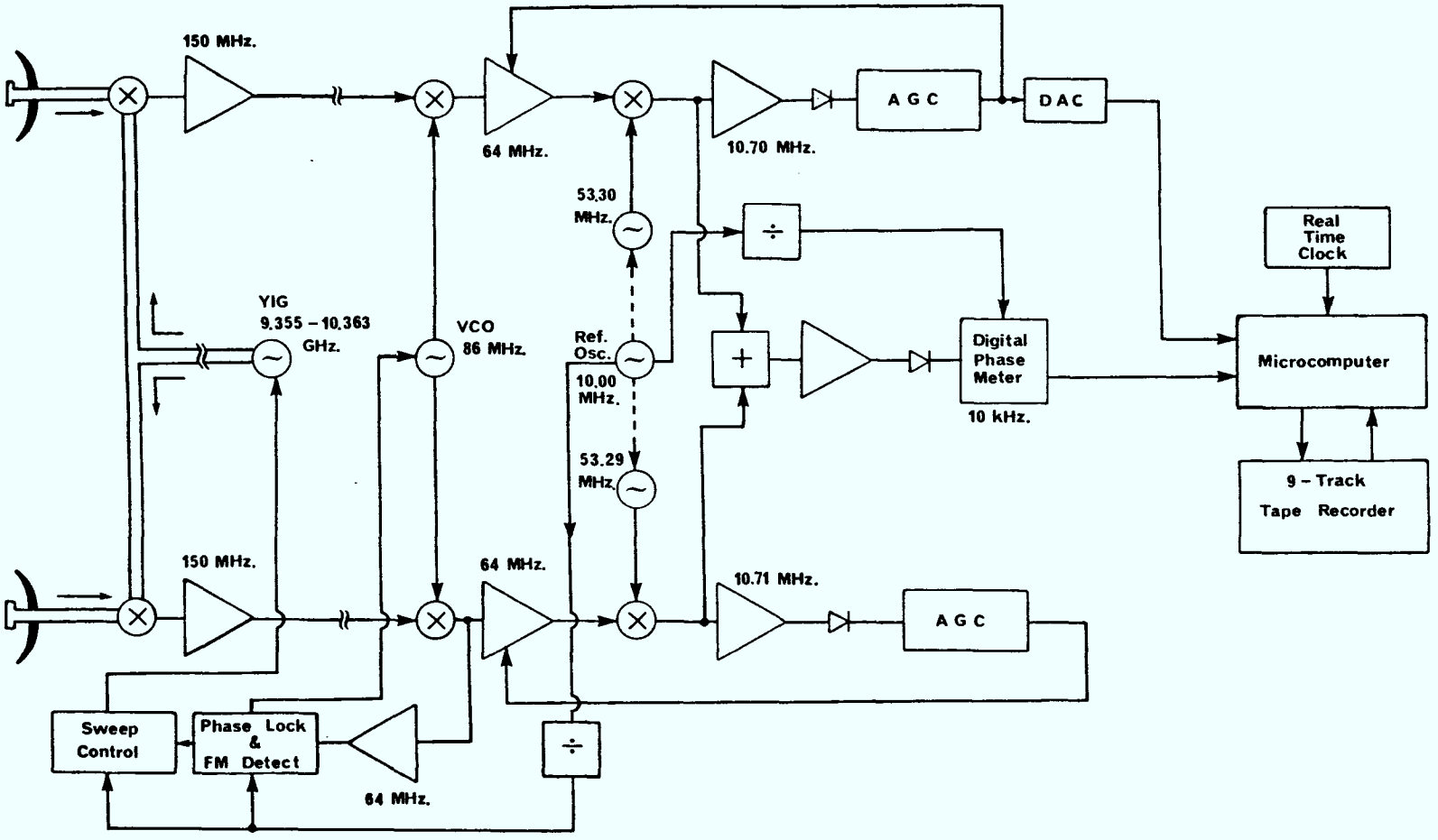

Fig. 2-1 Diagnostic System Receiver Block Diagram

2.2 The Propagation Path

The propagation path between Otter Lake, N.B., and Nictaux South, N.S., is an over-water path of length 80.375 km (Figure 2-2). This path was chosen by the telephone companies based on results from a previous test operated on a different link between Otter Lake, N.B., and Aylesford, N.S. The results from this previous experiment indicated the presence of a strong and persistent second ray path in addition to the normal ray path. This second ray path, which is present for a good proportion of the time, was believed to be caused by a reflection from the sea (Webster, 1981).

The choice of the Otter Lake - Nictaux S. path, then, was primarily aimed at eliminating this sea reflection by appropriate terrain blockage. The path profile is shown in Figure 2-3a with the ray paths drawn for a constant refractivity gradient, dN/dh, of -40 NU/km (corresponding to k = 1.34). The path profile for the Otter Lake to Aylesford link is shown in Figure 2-3b for comparison. It is observed that for the present link, the sea reflection is blocked by the North Mountain at least under normal conditions. Assuming an additional tree height of 12 m, the clearance for the reflected path at the North Mountain was estimated to be $-F_1$ at a frequency of 10 GHz, where F_1 is the radius of the first Fresnel Zone.

Further ray tracing was performed on the propagation path using different values of the refractivity gradient and three representative cases are shown in Figure 2-4. A few

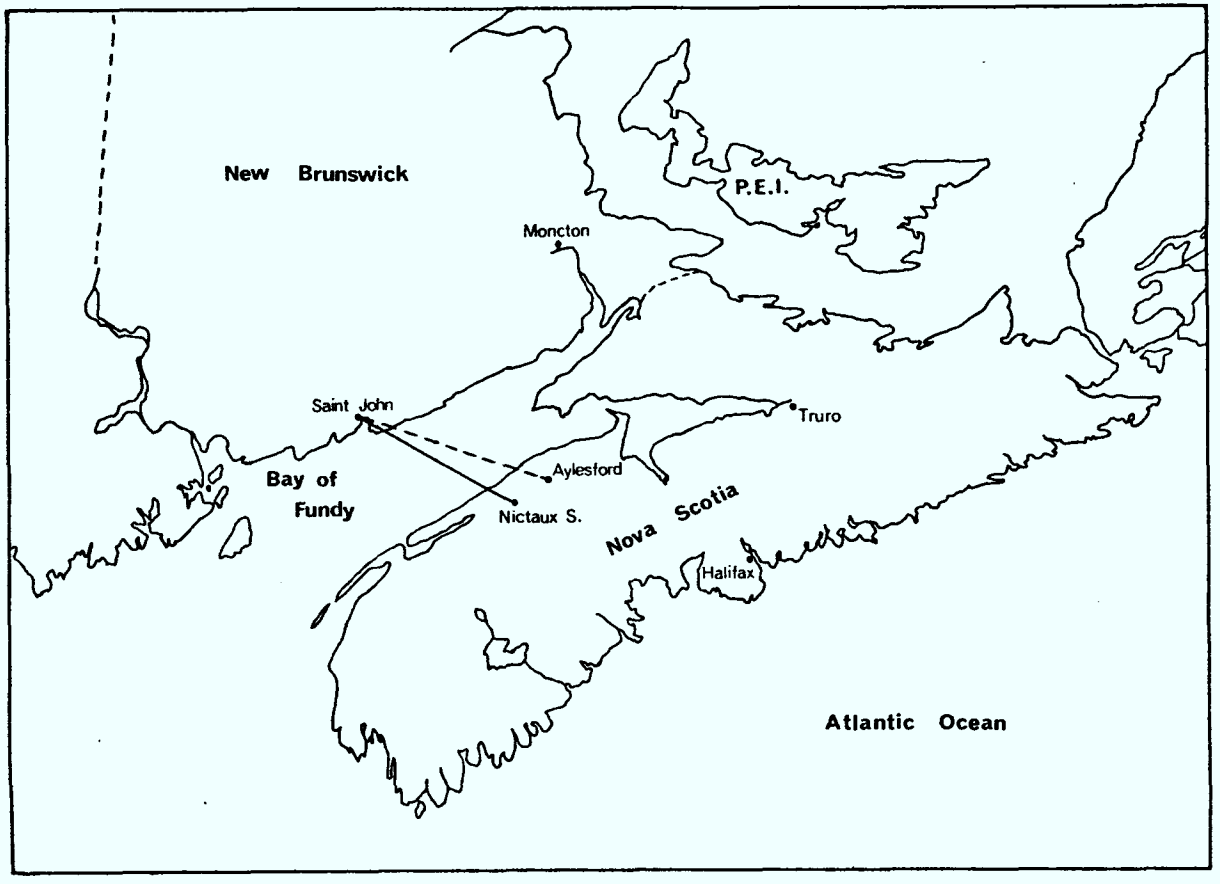

Fig. 2-2 The Propagation Path across the Bay of Fundy

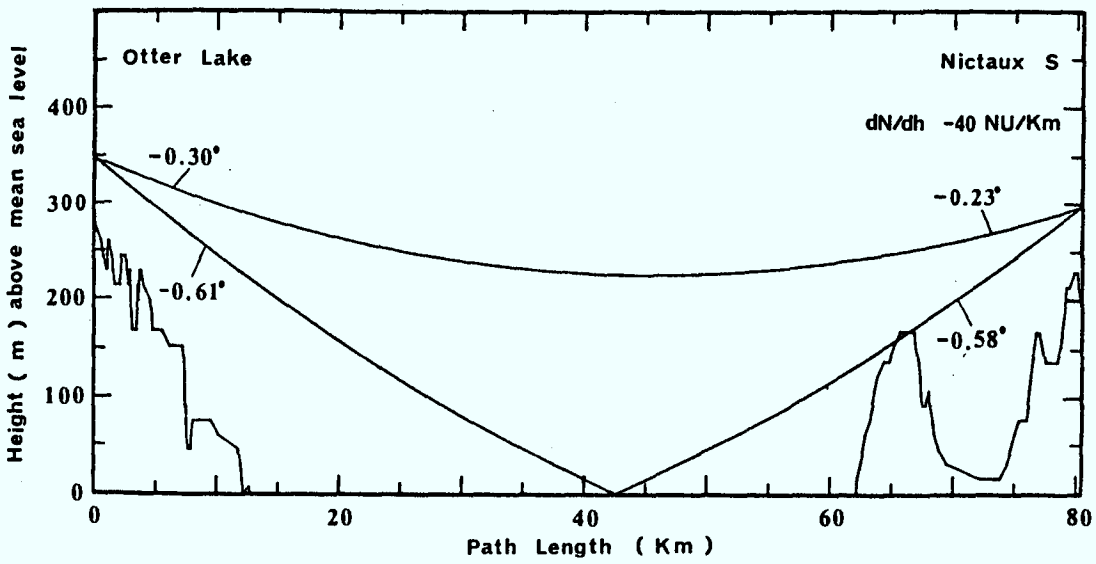

(a)

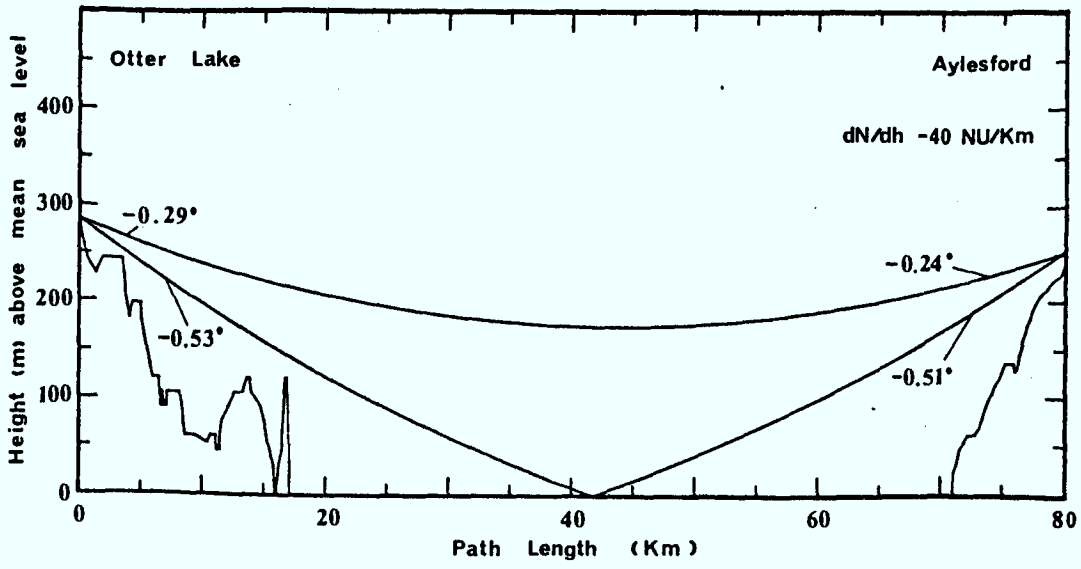

(b)

Fig. 2-3 Path Profiles of the Experimental Links;
(a) Otter Lake to Nictaux South, 1981
(b) Otter Lake to Aylesford, 1980

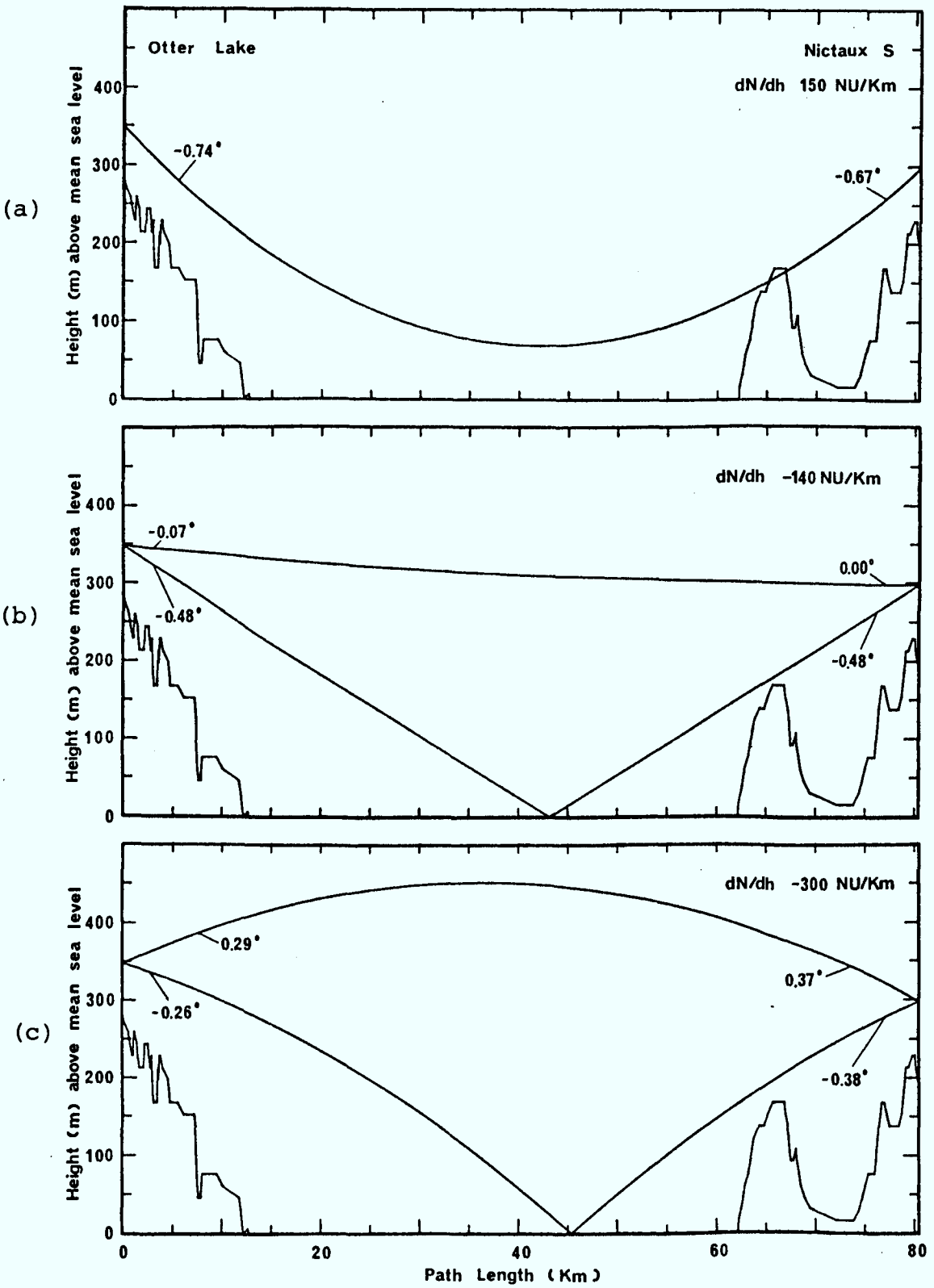

Fig. 2-4 Ray Tracing for Otter Lake - Nictaux South link using various values of the Refractivity Gradient:
(a) dN/dh= 150 NU/Km
(b) dN/dh=-140 NU/Km
(c) dN/dh=-300 NU/Km

points should be noted here. Firstly, the two cases with fairly extreme dN/dh values of 150 and -300 NU/km (corresponding to k = 0.51 and -1.1 respectively) were estimated to be the limits of a 99% range of dN/dh values encountered on this path during the summer months (Segal, 1977). The second point to note is that the blockage for the sea reflection is adequate provided the value of dN/dh is greater than approximately -140 NU/km, at least under conditions of uniform refractivity gradients. These results are summarized in Figure 2-5 in which the amplitudes of the direct and reflected rays were estimated based on ray tracing while taking into account the diffraction losses due to the North Mountain, assuming a reflection coefficient of -0.3 at the diffracting edge (see Figure 2-6) and a perfect sea reflection (White, 1970). For a normal gradient of -40 NU/km, the received signal was thus estimated to be composed of a direct ray of 'normal' amplitude and a reflected ray from the sea which is roughly -27 dB in amplitude relative to the direct path, with a delay of approximately 4.5 nsec between the two rays.

2.3 The Digital Radio

The RD-3 Digital Radio used by N.B. Tel. and M.T. & T. in the test hop is a part of the Northern Telecom DRS-8 Digital Radio System. The radio was designed to carry a 91.04 Mb/s bit stream (two DS-3 signals of 44.736 Mb/s each) over a 40 MHz (RF bandwidth) channel. The modulation

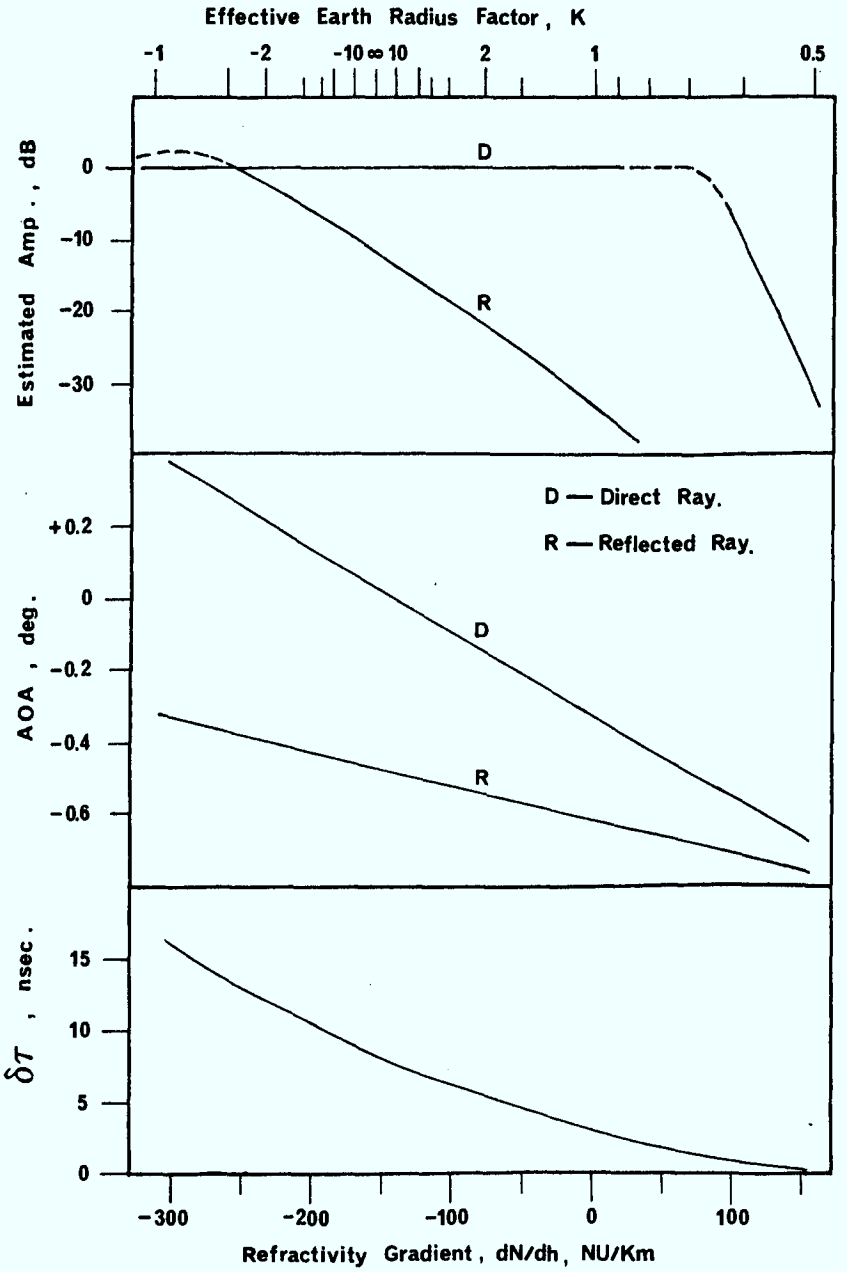

Fig. 2-5 Estimated Ray Path Parameters under Conditions of Uniform Refractivity Gradients

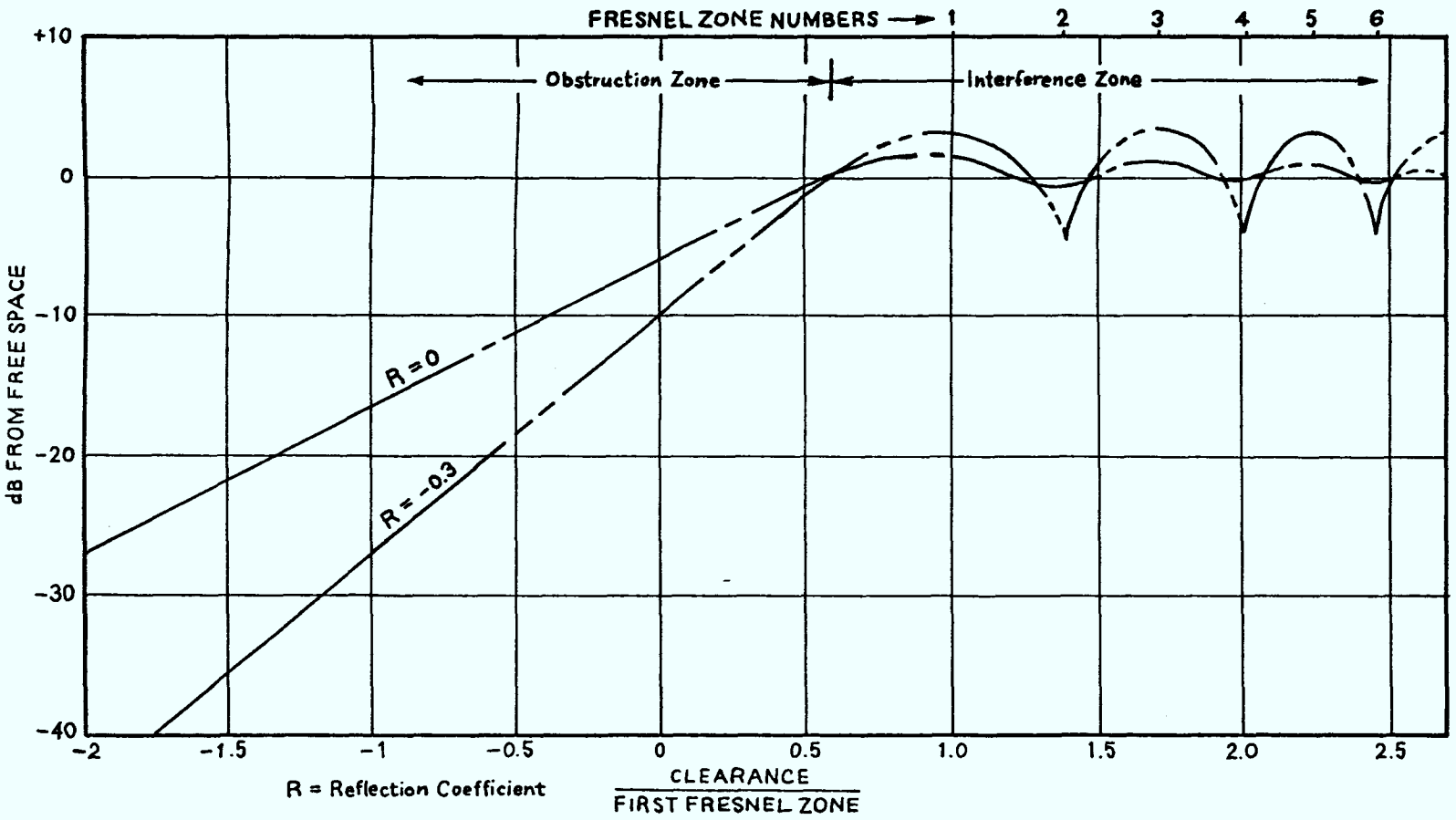

Fig. 2-6 Blockage Effect - Fresnel Zones

employed was Quadrature Partial Response Signaling (QPRS) which provided a signaling speed of better than 2 b/s per Hz. Protection against outages was provided in terms of both frequency and space diversity. The Main and Protection channel frequencies used in the test were 7.78611 GHz and 7.86759 GHz respectively. As for the space diversity protection, an adaptive in-phase IF combining technique was used. This combined signal was then conditioned by a linear delay equalizer and an adaptive linear amplitude equalizer before it was fed to the demodulator. The outputs from the demodulators of the Main and Protection channnels were fed to a CE-4B Automatic Protection Switch. Finally, one of the DS-3 signals from the protection switch was monitored by an HP-3782 Error Detector which performed Bit-Error-Rate (BER) measurements on the signal.

Two recording mediums were used in the experiment. The first is a 6-channel paper chart recorder that was operated continuously. The parameters recorded include the AGC levels of the Main, the Diversity, and the combined signals, the Eye-Voltage, and the Adaptive Equalizer Stress Voltage of the Protection channel, together with the Eye-Voltage of the Main channel. The other recording medium used was a digital tape recorder that recorded the above parameters plus the Sync-loss, BER, and the IF-Spectrum during periods when outages were observed on the digital radio.

The antennas employed in the digital radio test were 12-ft parabolic antennas with antenna gains of 46.8 dB. The antenna beamwidths were 0.73 deg between 3 dB points or 1.17 deg between 10 dB points. The transmit antenna at Otter Lake was mounted 79 m above ground and the receive antennas at Nictaux South were mounted at 79 m and 55 m above ground respectively for the Main and Diversity channels.

3. OBSERVATIONS AND RESULTS

3.1 General Considerations

The diagnostic system was operated during the period from 31st July to 3rd September totalling 809 hours. Events including equipment maintenance, power outages, and equipment malfunctions accounted for a total down time of 42 hours, or 5% of the time when no measurements were made. A time chart summarizing the fading events during the test is shown in Figure 3-1.

Out of the 767 hours in which measurements were made, 369 hours contained moderate to severe fading activities, or 48% of the time. To facilitate further discussions, an hour in which moderate to severe fading activities were observed will be referred to as a Fading Hour. In order to reveal a few important features, the data shown in Figure 3-1 was plotted in two different ways in Figure 3-2.

It can be seen in Figure 3-2a that fading hours were more frequently observed during the hours from 01:00 ADT to

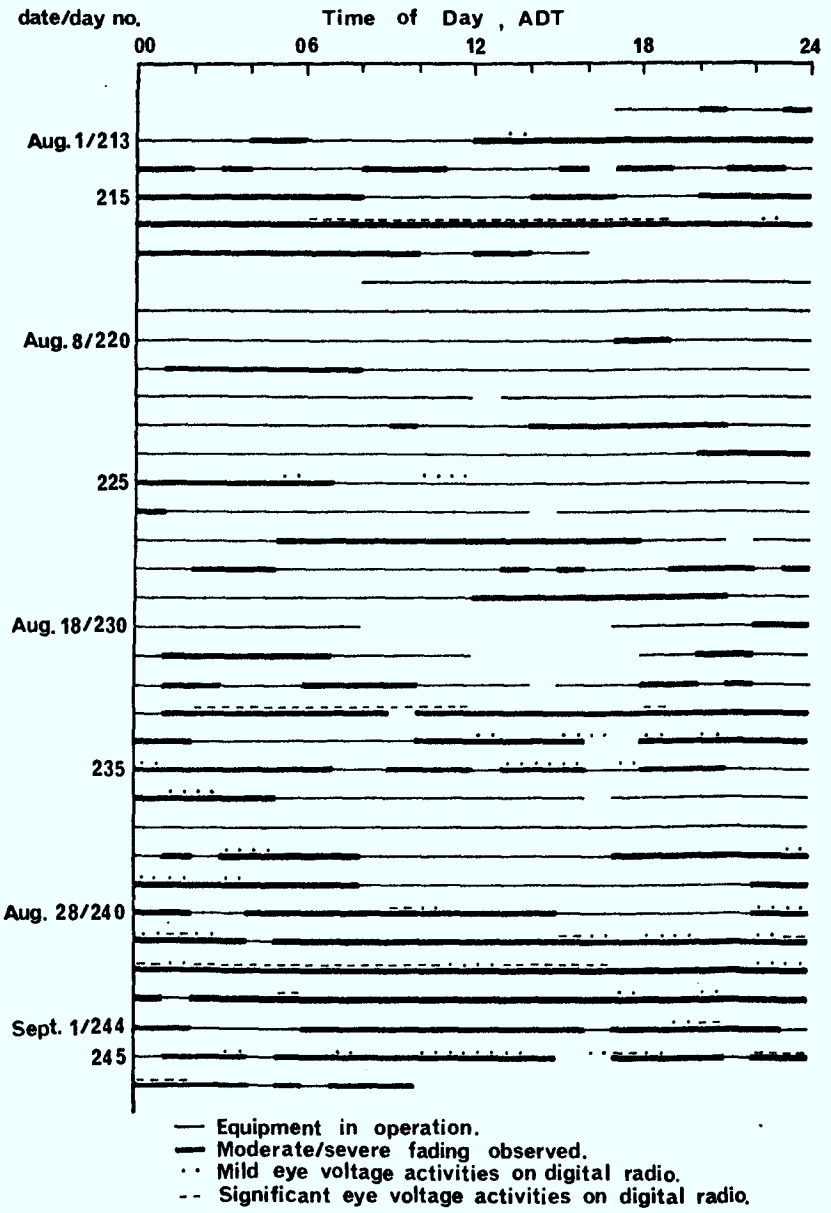

Fig. 3-1 Time Chart of Experimental Observations

(a)

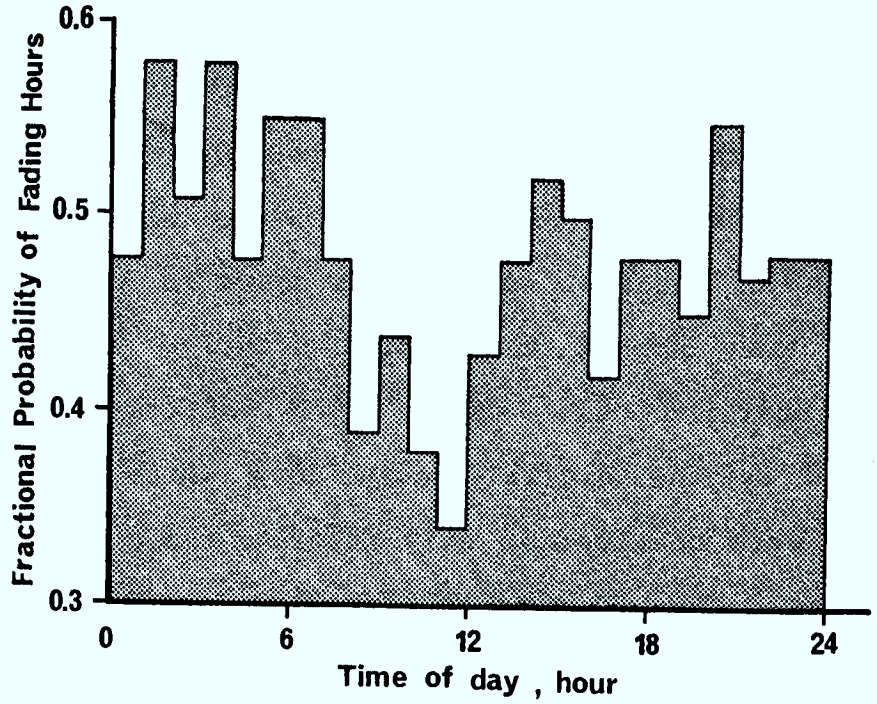

(b)

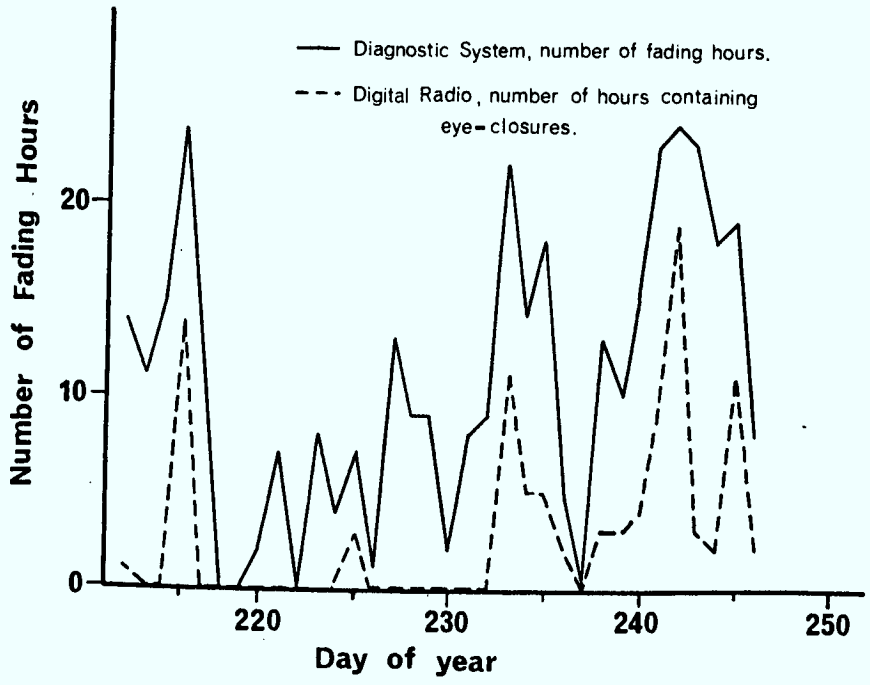

Fig. 3-2 Fading Statistics during the observation period;
(a) Probability of Fading Hours at different times of day
(b) Number of Fading Hours observed each day

07:00 ADT. The frequency of occurrence decreased during 08:00 ADT to 11:00 ADT and then increased again in the afternoon. Although the effect is not very pronounced, it is indicative of the presence of the types of fading associated with the diurnal heating and cooling of air masses. The second point of interest to note, as shown in Figure 3-2b, is that more than 50% of the fading occurred in three time periods totalling ten days. The effect was better illustrated by the digital radio test where most of the activities were observed in only five days during the 35-day test period. This latter observation suggests that the outages were mainly caused by anomalous fading associated with meteorological conditions that changed over periods of a few days.

Because of the large amount of data available, it was initially analysed by selecting representative days for three different categories, namely, quiet days, days with moderate fading activities but no bit errors on the digital radio, and finally, days with severe fading activities and significant BER's on the digital radio. The results in each case are presented in the following sections.

A few comments should be made here that concern the interpretation of the results presented in the following sections. The automated routine employed for the data analysis was developed to produce, from the raw sweep data, the amplitudes of the two strongest rays, the relative delay between these two rays, and the angle-of-arrival of the

strongest ray. Because of the nature of the algorithm used, insignificant or extraneous results will be produced under two particular situations. First, when the second ray is too low in amplitude or altogether non-existent, the relative delay estimate will be incorrect. Second, when the second ray path is of comparable amplitude to the strongest ray, the main path angle-of-arrival estimate will be incorrect. In these cases, a trial-and-error synthesis technique has to be used to estimate the angles-of-arrival of the ray paths. The reader is thus reminded that during periods of severe multipath fading, the main path angle-of-arrival results in the full day plots should be ignored. The results in all cases were plotted and not suppressed because they do give a good indication of the nature of the fading involved.

3.2 Quiet Day Results

The time period from 6th August to 8th August (days 218/219/220) was relatively calm in terms of fading activities and no BER was recorded on the digital radio. A typical sweep record from the diagnostic system is shown in Figure 3-3 together with the parameters for the received ray paths obtained by a synthesis technique. Two received ray paths were identified in the record and all the ray path parameters including the amplitudes, the angles-of-arrival, and the relative delay of 4.5 nsec fit in extremely well with the expected values as predicted in Section 2.2 and Figure 2-5.

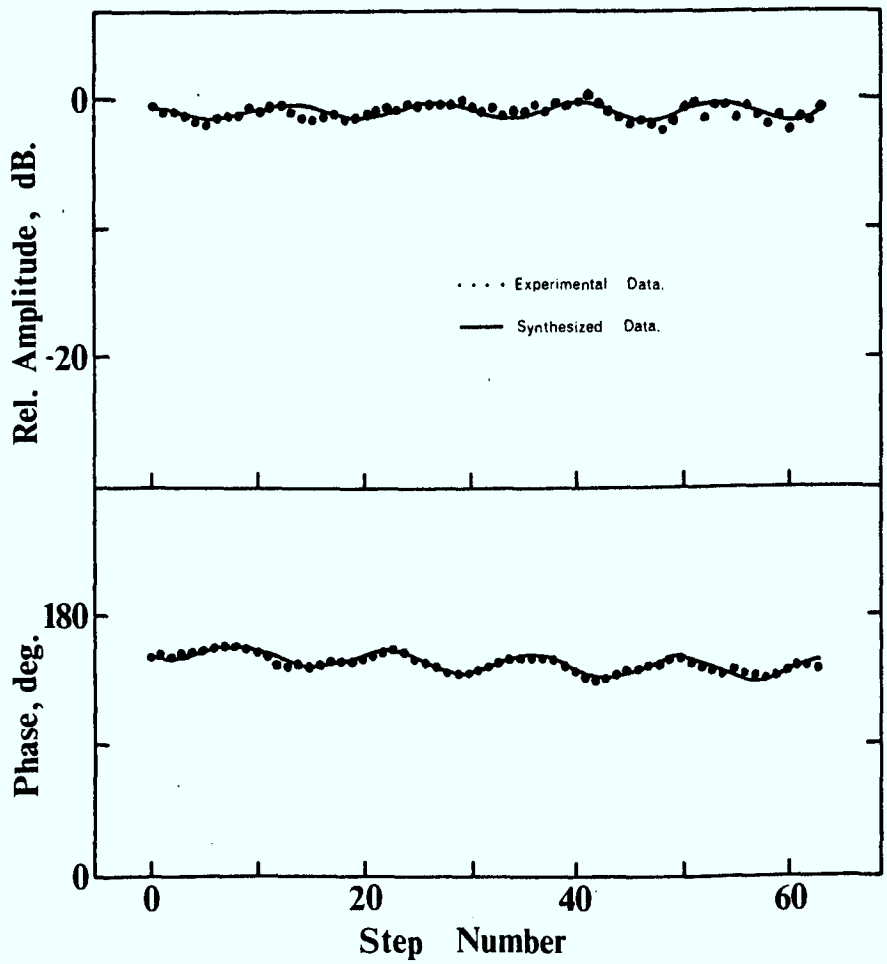

Rel. Ampl.,dB.	AOA°	$\delta\tau$, nsec.
-1.1	-0.25	-
-25.0	-0.50	4.5

Fig. 3-3 Typical Diagnostic System Sweep Record during a Quiet period - day 219, 00:00:05 ADT

The data in the above three days were analysed and some of the results are shown in Figures 3-4 and 3-5. The main path amplitude was observed in both figures to be relatively constant with little fluctuation (±5 dB) about the normal signal level. The second ray path was observed to be between -35 to -20 dB relative to the normal signal level with relative delays of between 3.5 to 5 nsec over most of the day. The variations in the main path angle-of-arrival (AOA) was observed to exhibit routine variations with ranges of ±0.13 deg (-0.15 to -0.4 deg) for days 218/219 and ±0.2 deg (-0.1 to -0.5 deg) for days 219/220 over each day. Also particularly interesting are the significant swings in the main path AOA observed at 23:00 ADT on day 219 with a range of almost 0.9 deg (+0.2 to -0.7 deg). A plot of the hour's data on an expanded scale revealed that the AOA actually changed from -0.65 to +0.2 deg in a time of less than 8 minutes.

To further illustrate the changes in the main path AOA observed during this period, variations of hourly average AOA's were plotted in Figure 3-6 for the days 218, 219, and 220. The range in the hourly averages was observed to be roughly 0.15 deg. To look at AOA variations from a statistical viewpoint, AOA probability distribution curves were computed and shown in Figures 3-7 and 3-8. The data sample for computing these curves was obtained from 32693 sweep records collected during quiet conditions over days 218, 219, 220, 227, 228, and 229. The AOA probability

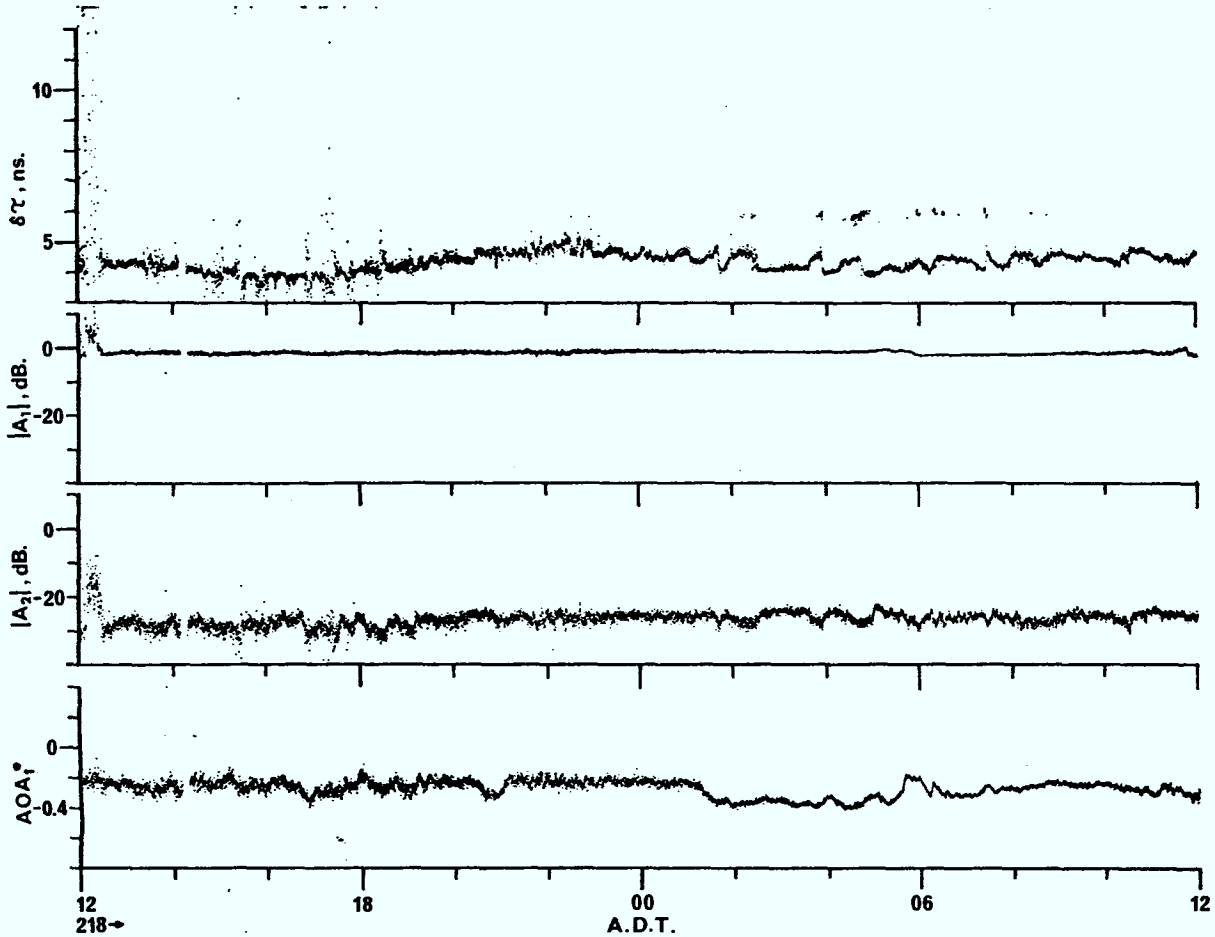

Fig. 3-4 Received Signal Ray Path Parameters on 6th and 7th August, days 218/219

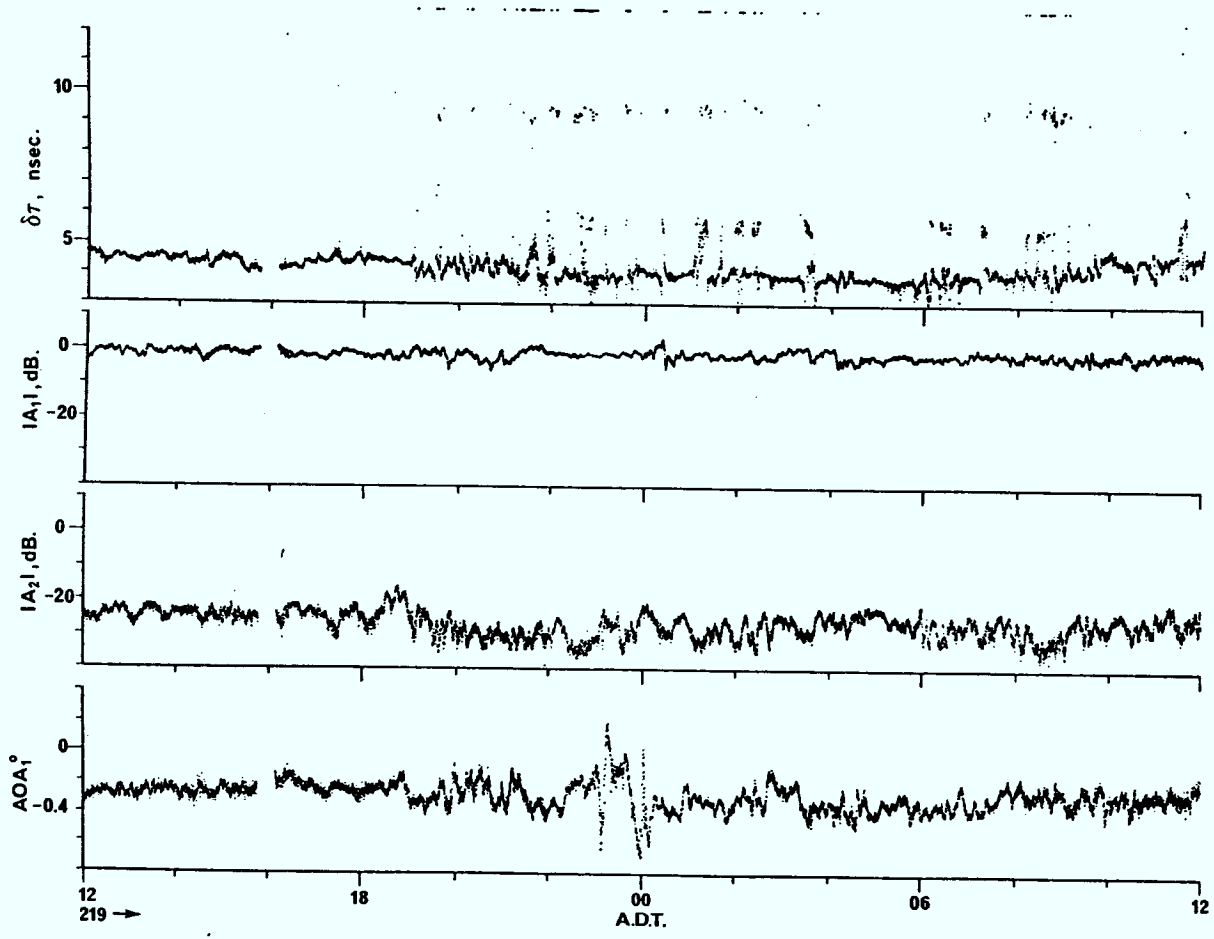

Fig. 3-5 Received Signal Ray Path Parameters on 7th and 8th August, days 219/220

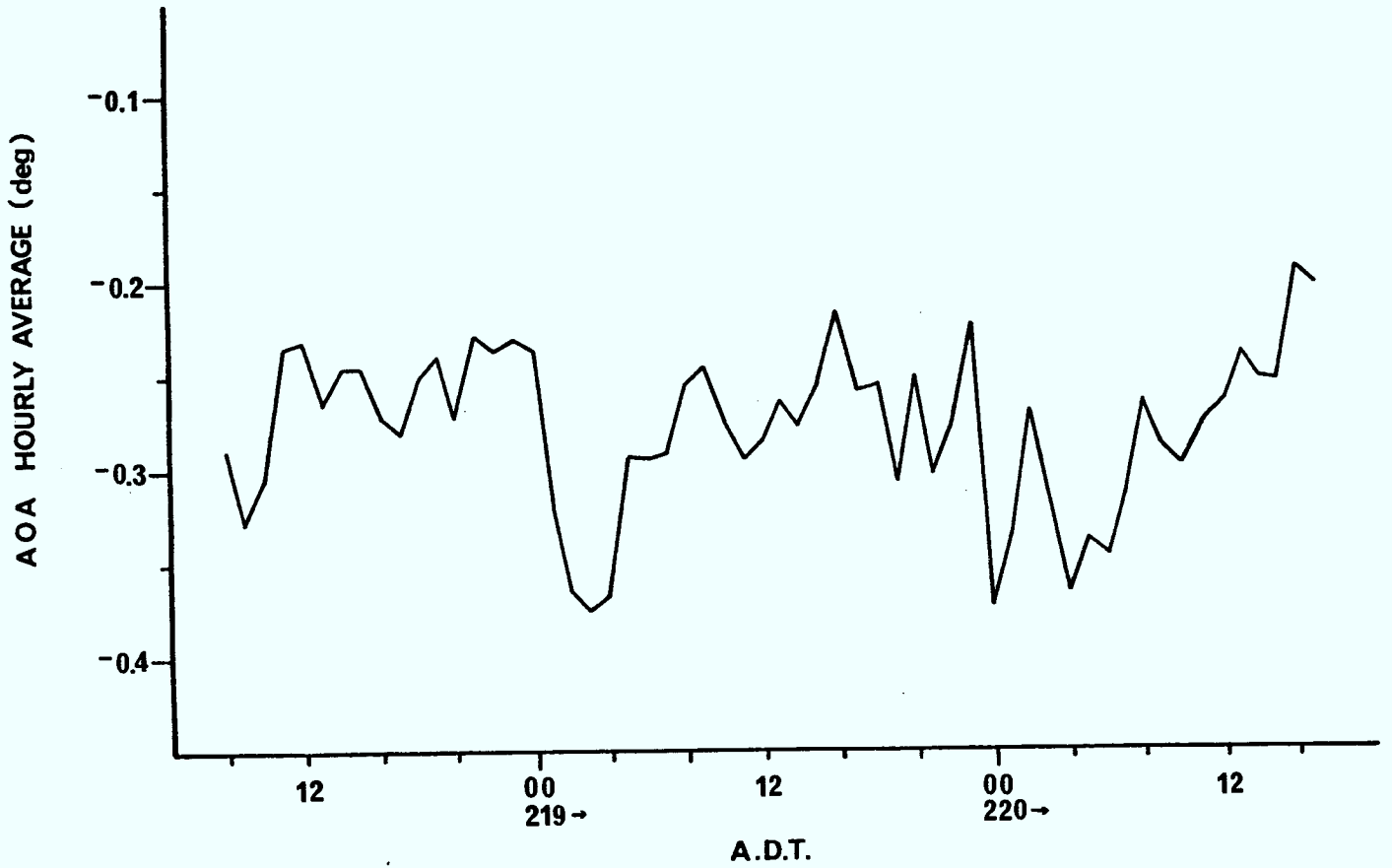

Fig. 3-6 Variations of Hourly Average AOA from 6th to 8th August, days 218/219/220

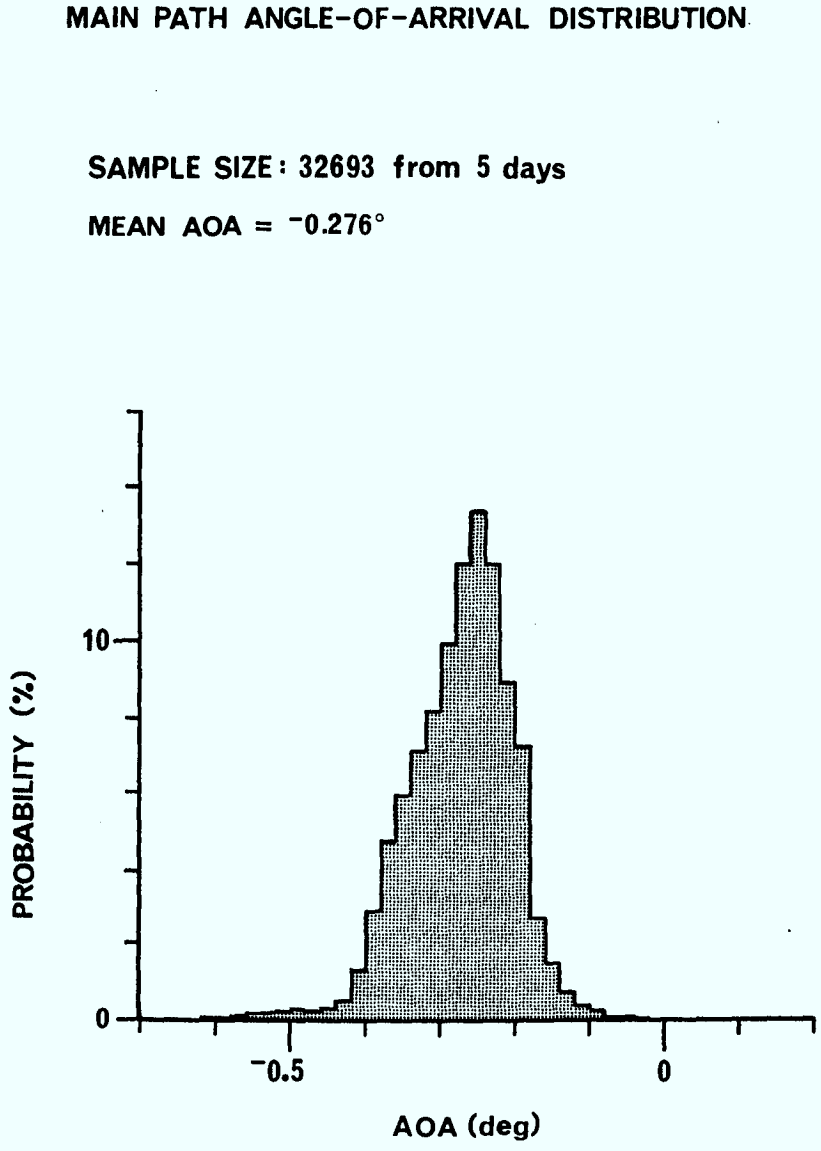

Fig. 3-7 Probability Distribution of the Main Ray Path Angle-of-Arrival under quiet conditions

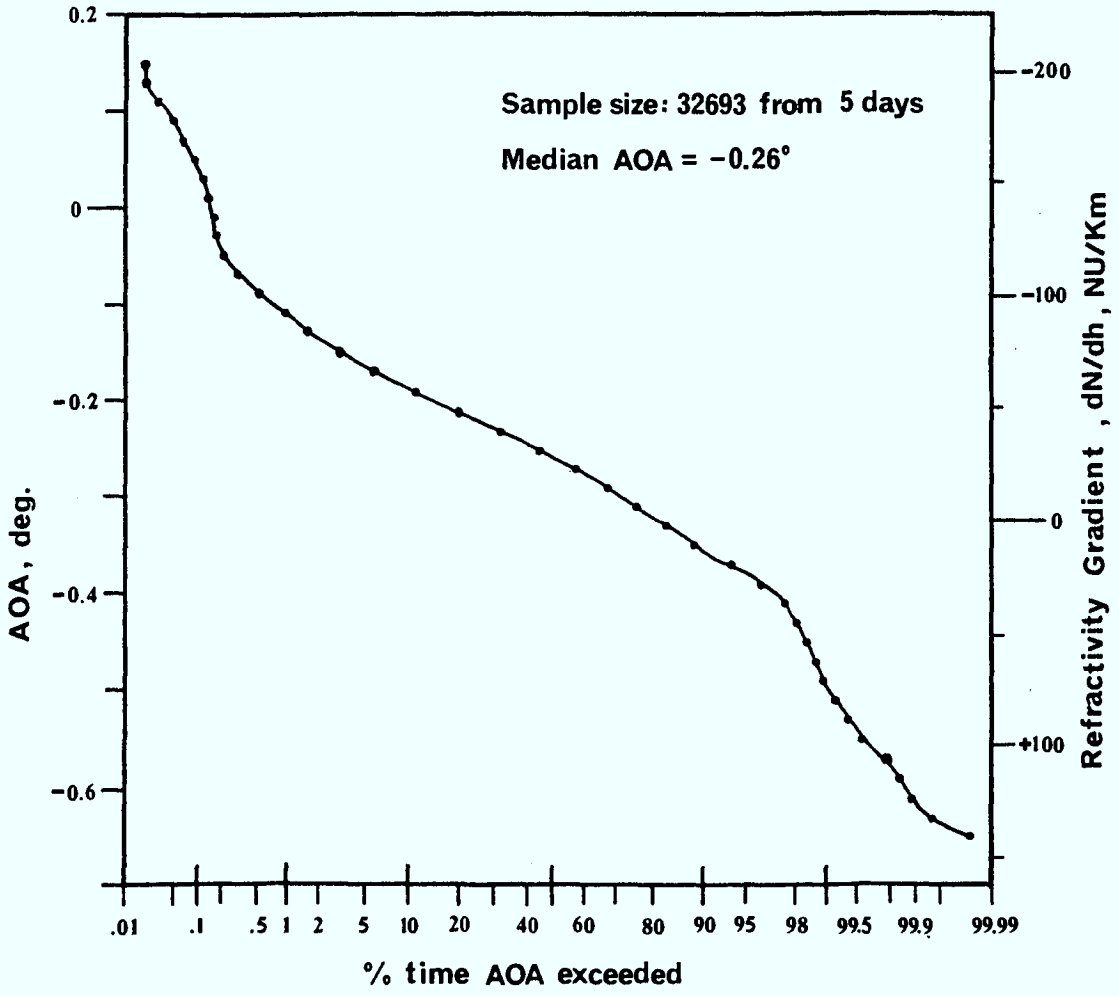

Fig. 3-8 Cumulative Probability Distribution of the Main Ray Path Angle-of-Arrival under quiet conditions

distribution in Figure 3-7 shows a skewed structure with a long tail for lower AOA values and a range of at least 0.6 deg. This is further illustrated in Figure 3-8 where a 99.9% range of AOA is $\sim$0.7 deg. Assuming a constant gradient refractivity profile with a ground refractivity of 300 NU and a median or 50% cumulative probability value of -40 NU/Km for the refractivity gradient, the AOA values may be related to dN/dh values for this particular propagation path and the result is shown on the scale to the right of Figure 3-8. The 99.9% range then corresponds to the range of dN/dh values from approximately -170 to +130 NU/Km, at least for the five days from which the data sample was taken.

3.3 Days with Moderate Fading Activities

Moderate fading activities were observed on 15th, 16th, and 17th August (days 227, 228, and 229). Again no BER occurred on the digital radio during this period of time. Some of the results from these days are shown in Figures 3-9 and 3-10.

As was the case for the quiet conditions, two received ray paths were identified. However, there were considerable differences as regards the characteristics of the two ray paths. From 14:00 ADT to 20:00 ADT on day 227, the second received ray was observed to fluctuate in amplitude and at times increased to more than -10 dB relative to the amplitude of the main ray, with the relative delay varying considerably between 4.5 nsec and 6.5 nsec.

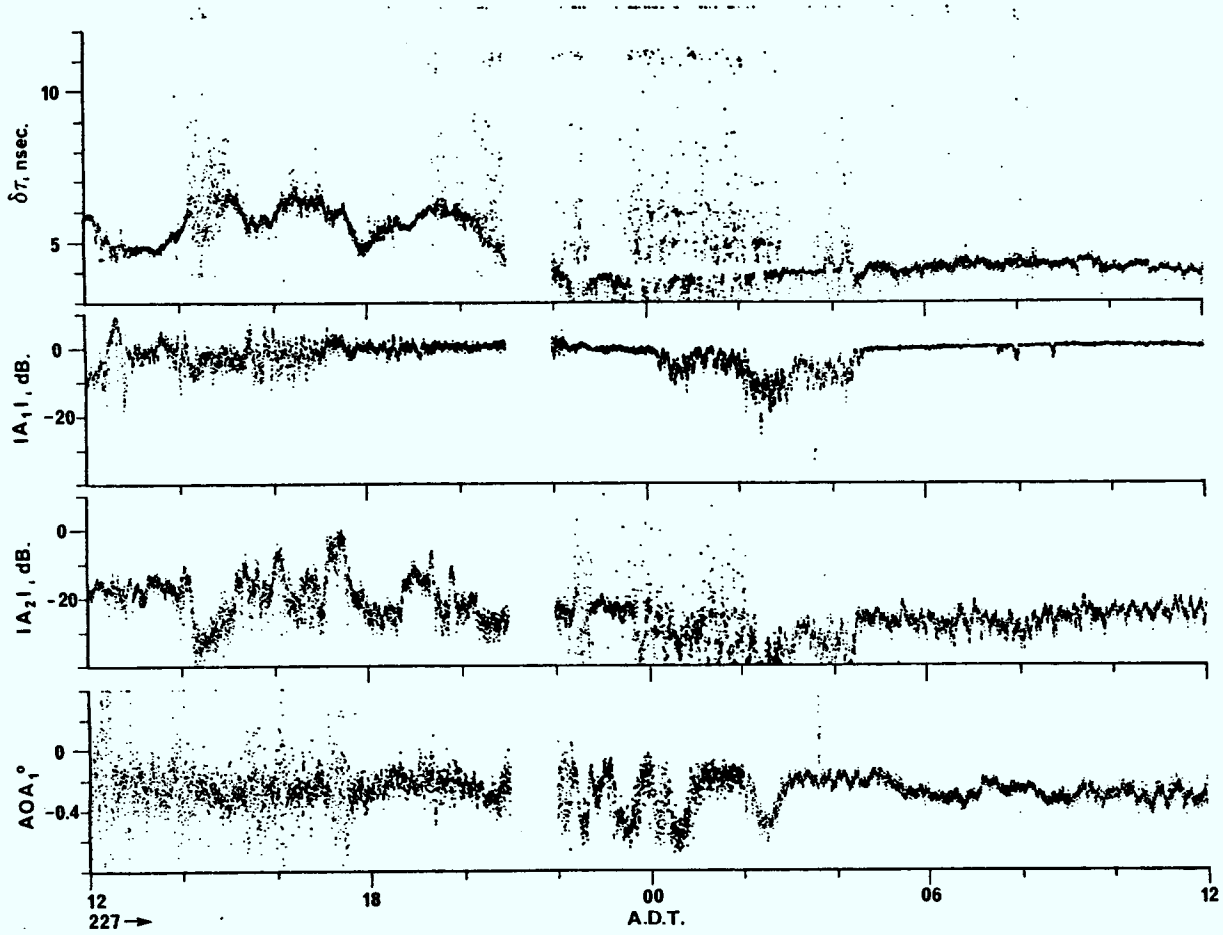

Fig. 3-9 Received Signal Ray Path Parameters on 15th and 16th August, days 227/228

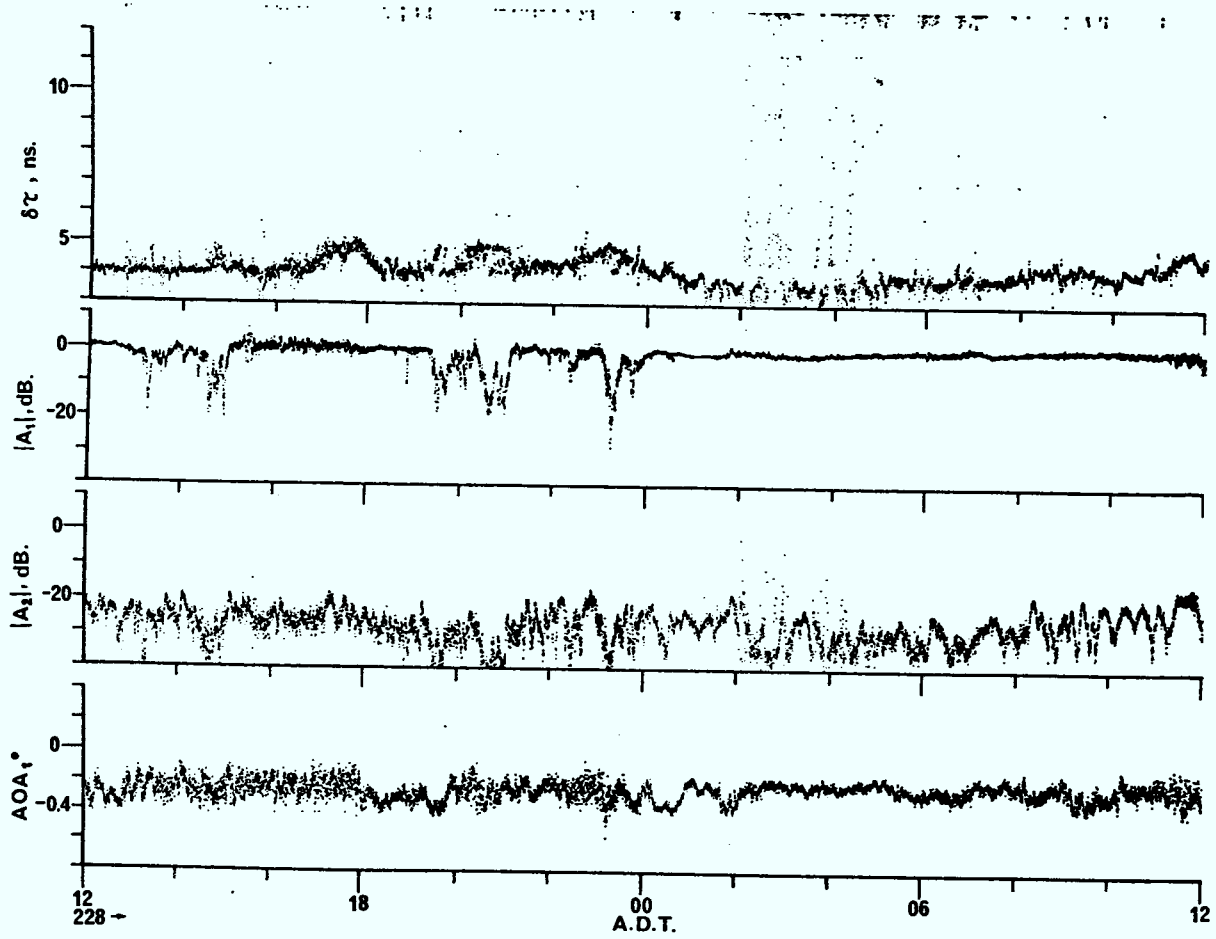

Fig. 3-10 Received Signal Ray Path Parameters on 16th and 17th August, days 228/229

Also prominent in Figures 3-9 and 3-10 are the behaviours observed on day 228 during the periods 00:00 ADT to 05:00 ADT, 13:00 ADT to 15:00 ADT, and again during 19:00 ADT to 23:00 ADT. The amplitudes of the two received rays faded in concert with each other by more than 10 dB on more than a few occasions. Rain fading is believed to be the cause of the above observations as fairly heavy rain was observed on day 228. The digital radio was observed to operate well during the above periods of substantial rain fading.

3.4 Days with Severe Fading Activities

The worst fading period during the experiment occurred on 30th August (day 242) when unacceptably high BER's were also observed on the digital radio. As shown in Figure 3-1, activities on the digital radio started in the evening on day 241 and continued well into late afternoon on day 242.

One set of 'typical' sweep data during such fading periods is shown in Figure 3-11. The amplitude record displayed a series of nine nulls across the 1 GHz band (due to destructive interference of the two received rays with a delay of 9.2 nsec between ray paths) with fade depths of more than 20 dB below the normal signal level. In actual fact, for two received ray paths, the number of nulls contained within a 1 GHz band is numerically equal to the relative delay in nano-seconds between the two ray paths. An important consequence is that for any wideband communication

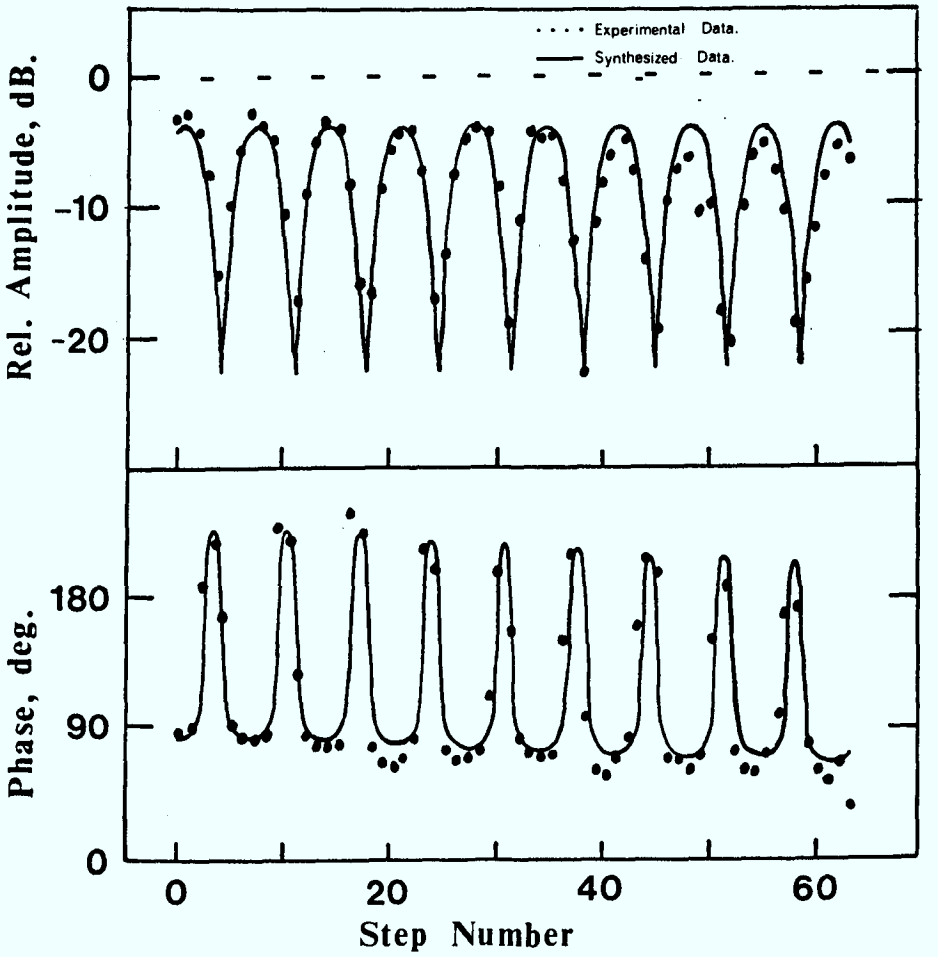

Rel. Ampl., dB.	AOA°	$\delta\tau$, nsec.
-10.8	0.02	-
-8.9	-0.43	9.2

Fig. 3-11 Typical Diagnostic System Sweep Record during a severe fading period - day 242, 10:04:52 ADT

system (e.g. RD-3 radio has 40 MHz RF bandwidth), the probability of an in-band null (and hence in-band amplitude and group delay distortion) occurring within the radio bandwidth increases directly as the relative delay between the two received ray path increases. Since digital radios are known to be vulnerable to in-band distortion, the existence of long delays between ray paths are to be avoided in the radio path design.

In addition to the relative delay of 9.2 nsec shown in Figure 3-11, the other characteristics of the received ray paths are also noteworthy. First, the normal ray (the one that arrived first in time at the receiver) was observed to fade by more than 10 dB relative to the normal signal level while the AOA was elevated above the normal AOA (+0.02 deg versus -0.25 deg). The second ray path, on the contrary, actually exceeded the main ray in amplitude (-8.9 dB relative to normal signal level) while also showing an elevated AOA.

The data for the days 241 and 242 were processed and some of the results are shown in Figures 3-12 and 3-13. The prominent feature observed in these figures is the relative delay characteristics. A delay of greater than 6 nsec was observed over most of the two day period and at times it increased to as high as 10.5 nsec. Again at least two ray paths were detected over most of the day. The main path amplitude was seen to fluctuate violently and at times faded by more than 20 dB relative to the normal signal level. The second ray path also fluctuated considerably and at times

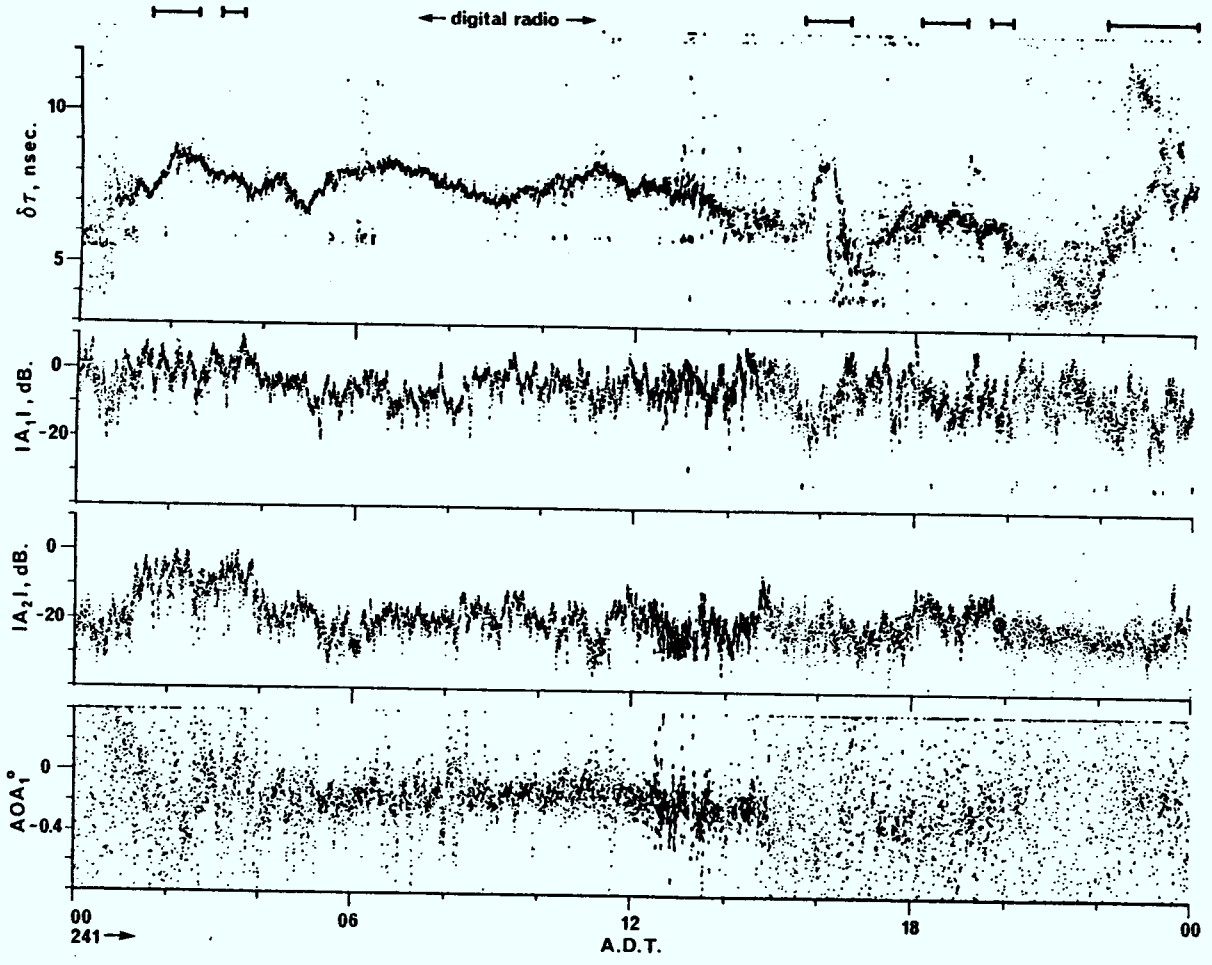

Fig. 3-12 Received Signal Ray Path Parameters on 29th August, day 241

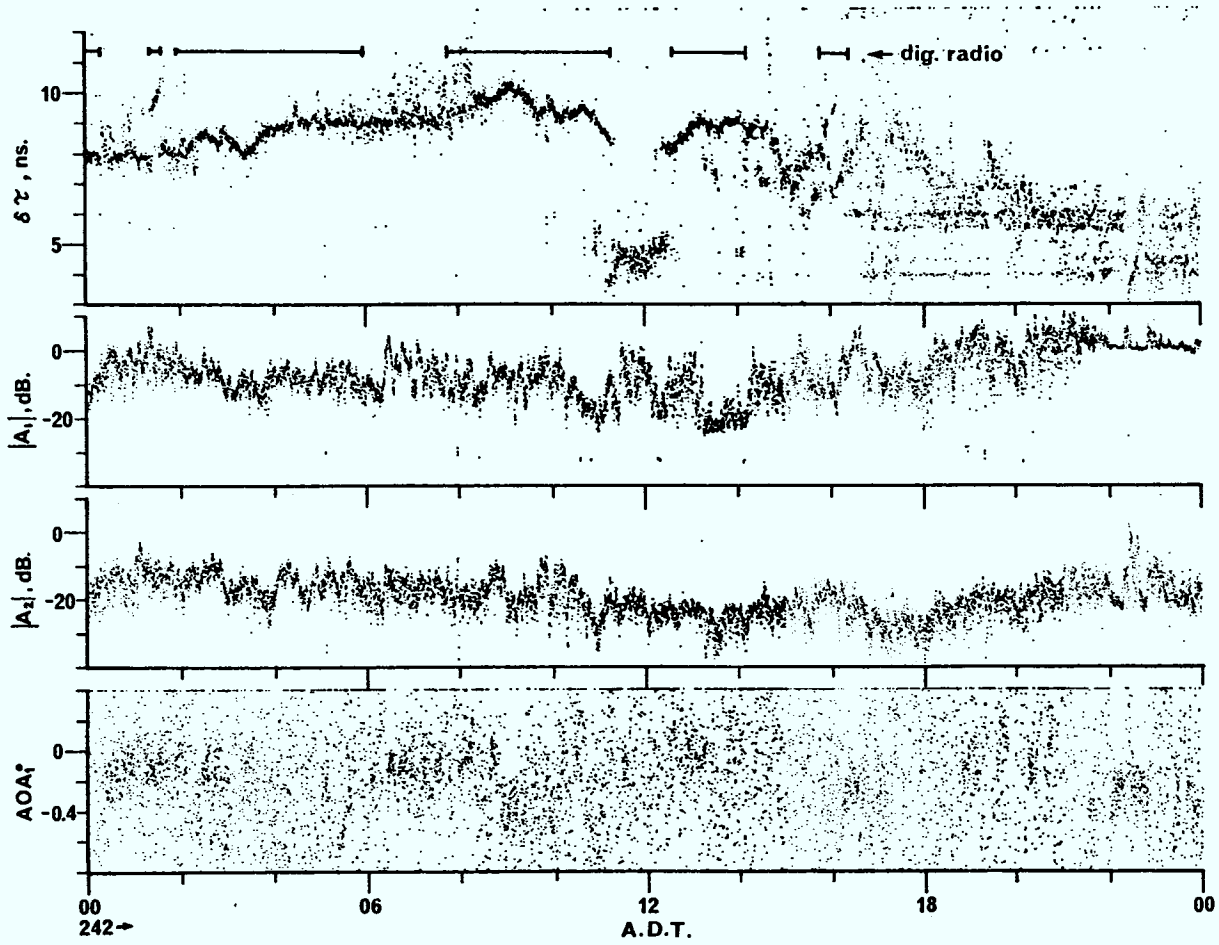

Fig. 3-13 Received Signal Ray Path Parameters on 30th August, day 242

increased to greater than -5 dB relative to the normal signal level, resulting in a small differential amplitude between the two received rays which produced extremely deep fades.

The reader is reminded here that although the parameters for only two ray paths were presented in the above results, it was not intended to imply that only two ray situations arise. In actual fact, some raw data records inspected show evidence of the existence of at least three received ray paths. As explained earlier, the automated data analysis routine presently employed was designed to identify the two strongest received rays and although it worked very well, it is neither complete nor exhaustive. More thorough analysis, which requires a lot of manpower, time, and computing facilities, is very much an on-going process.

In assessing the performance of the digital radio during this period of severe fading, the time intervals when numerous complete closures of the receiver eye-pattern were observed on the digital radio were noted and plotted in Figures 3-12 and 3-13. The Eye-Voltage was used as the criterion because it is a very good indication of the quality of the digital signal at the demodulator output, and hence a good indication of the BER to be expected on the digital radio. In studying Figures 3-12 and 3-13, it appeared that outages on the digital radio were mainly caused by one or a combination of the following conditions, namely, (i) a long relative delay of $\gtrsim$ 8 nsec, and (ii) a small differential amplitude between the two received rays.

In an effort to further investigate the above-mentioned causes of digital radio outages, probability distribution curves were computed for the differential amplitude and the relative delay during three different periods and these are shown in Figure 3-14. In Figures 3-14a and b, the distributions were computed for 17th August (day 219) which is a quiet day in terms of fading activities. The relative delay, in such cases, was observed to center around a median value of $\sim$ 4.5 nsec with little spread. The same is true of the differential amplitude between the two strongest rays with a median value of $\sim$ 25 dB. Figures 3-14c to f are distributions computed for the severe fading day 242, with c and d computed using data from the hours when little or no outages occurred on the digital radio, and e and f computed using data from the hours when severe outages were observed. The distributions with large relative delay and small differential amplitude associated with digital radio outages are well displayed in the comparison.

3.5 Miscellaneous Observations

Up to this point, the results presented in the report were mostly concerned with two received ray paths one of which originated from a reflection off the sea. The relative delay associated with such a reflected ray was observed to range from 3.5 to 10.5 nsec. It is important to point out here that multipath fading with short relative delay was also observed during the experiment on more than a few occasions.

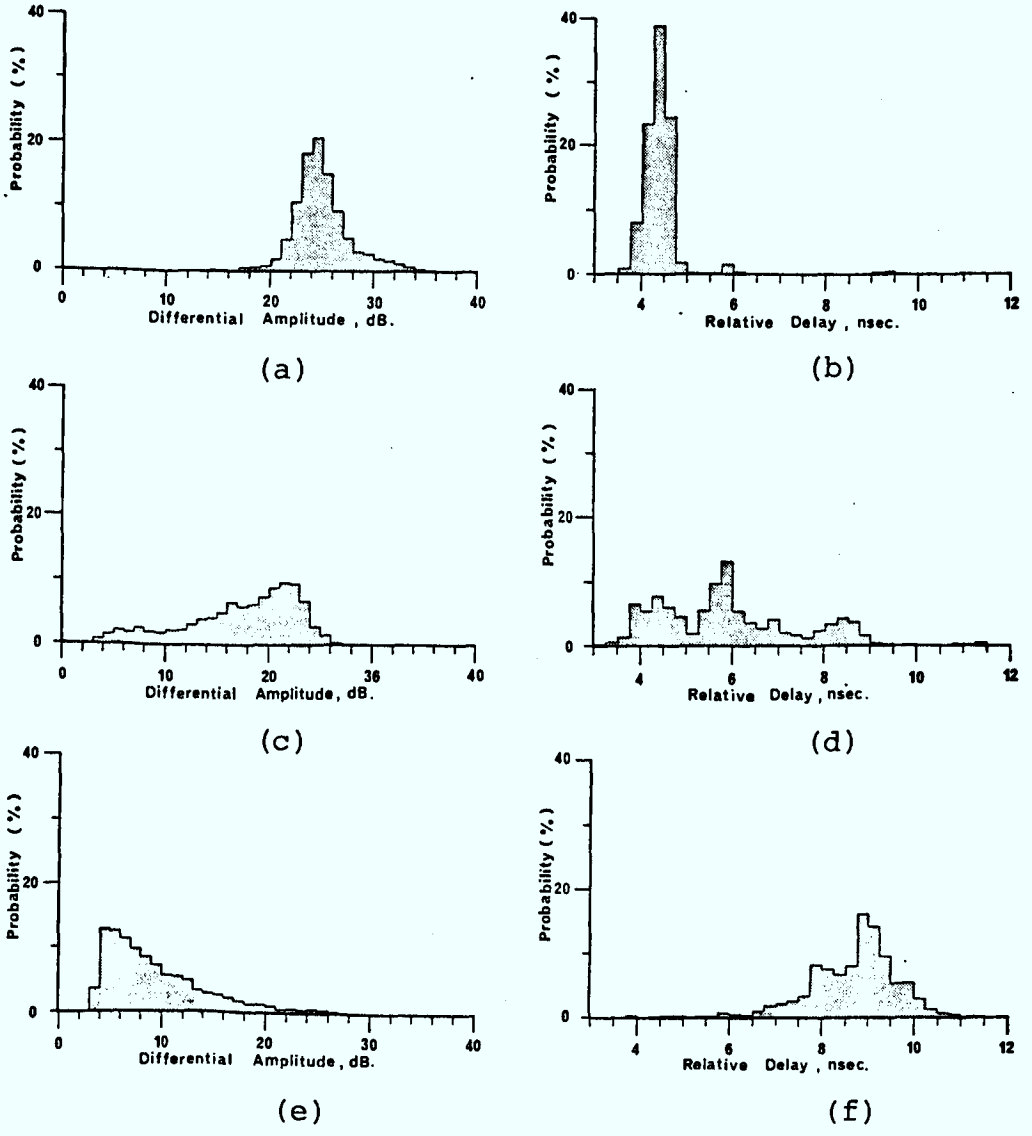

Fig. 3-14 Probability Distributions of the Differential Amplitude (a,c and e) and the Relative Delay (b,d and f) under various fading conditions;
(a) and (b) - Distributions for a quiet day with no errors on digital radio (day 219)
(c) and (d) - Distributions during active fading hours of day 242 when small or no BER's were observed on digital radio
(e) and (f) - Distributions during active fading hours of day 242 when significant BER's were recorded on digital radio

These additional ray path(s) are believed to be atmospheric in origin and in many cases occur in addition to the reflected ray from the sea.

One example of such atmospheric multipath fading occurred on 4th August (day 216) and six minutes of consecutive records are shown in Figures 3-15a, b, and c. The sea reflection in this example was non-existent and instead a very fast changing second path with a relative delay of around 0.5 nsec was observed, as evident during the time between 01:56:55 ADT to 01:57:55 ADT, and again from 01:59:55 ADT to 02:01:15 ADT in Figure 3-15. It should be pointed out that significant changes were observed between sweeps which were taken every 10 sec, implying that conditions were changing much faster than 10 seconds. The amplitude of this second path also was changing rapidly and at times it was observed to be within ± 1 dB of the amplitude of the main path (e.g. at 02:00:05 ADT), thus resulting in extremely deep fades of more than 35 dB below the normal signal level. A more thorough analysis of this type of multipath is anticipated in the near future.

4. SUMMARY AND DISCUSSION

A representative cross section of the types of fading observed on a propagation path across the Bay of Fundy was presented in this report. The 80 Km over-water path from Otter Lake to Nictaux South exhibited a higher than normal probability of fading (48% of the time by hour contained

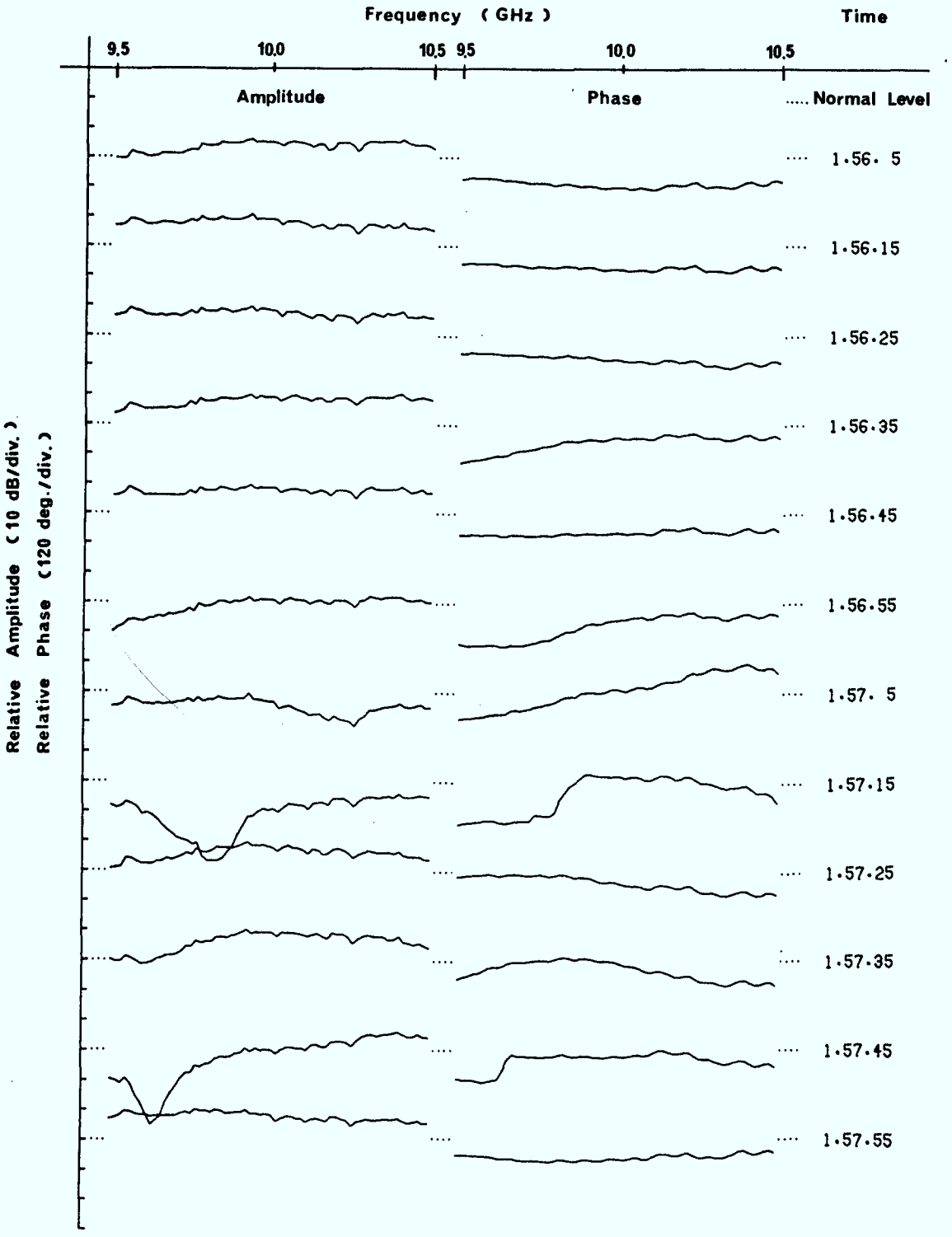

Fig. 3-15(a) Consecutive Sweep Records from Diagnostic System on 4th August (day 216) showing fast fading with short relative delay

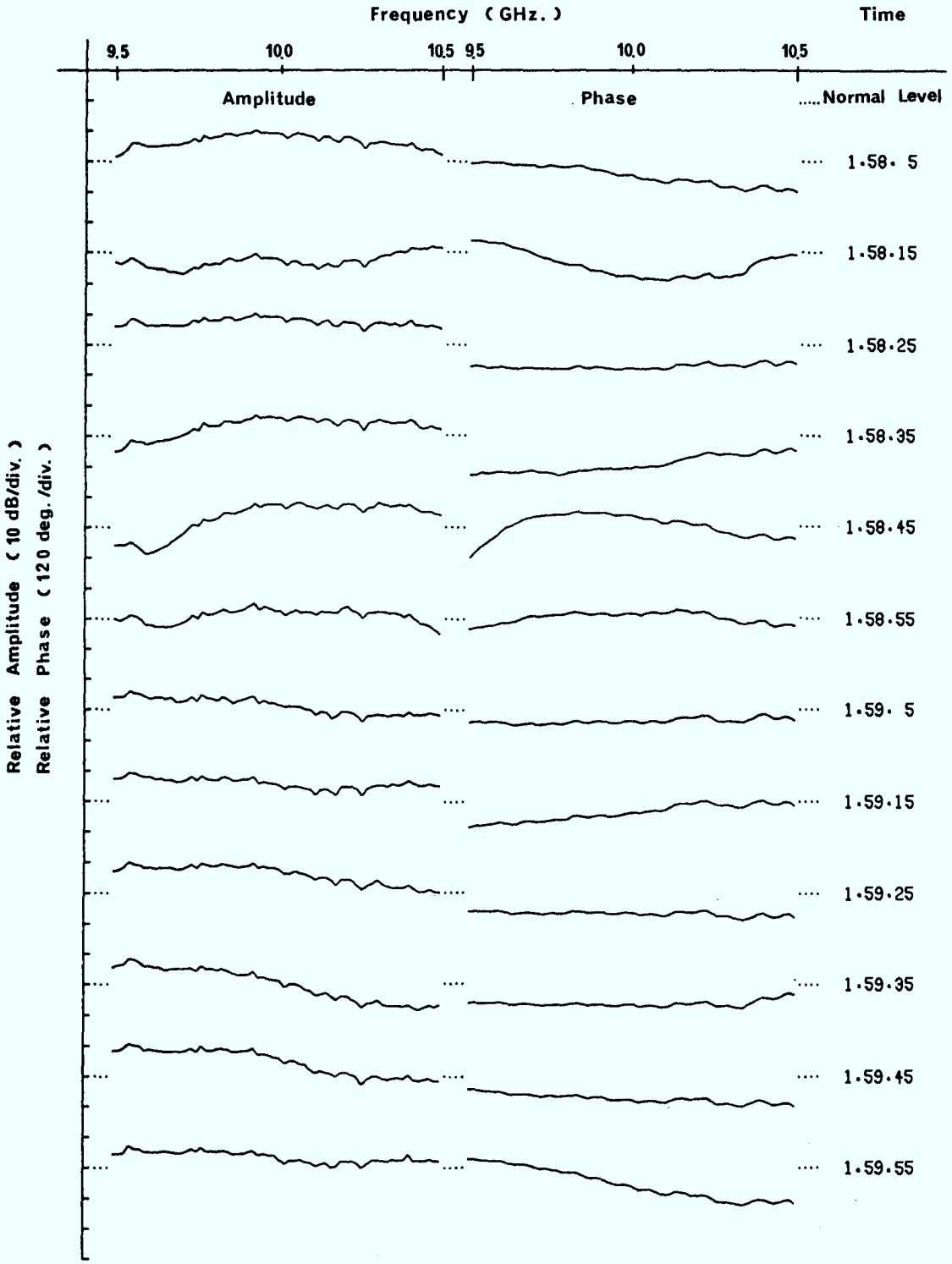

Fig. 3-15(b) Consecutive Sweep Records from Diagnostic System on 4th August (day 216) showing fast fading with short relative delay

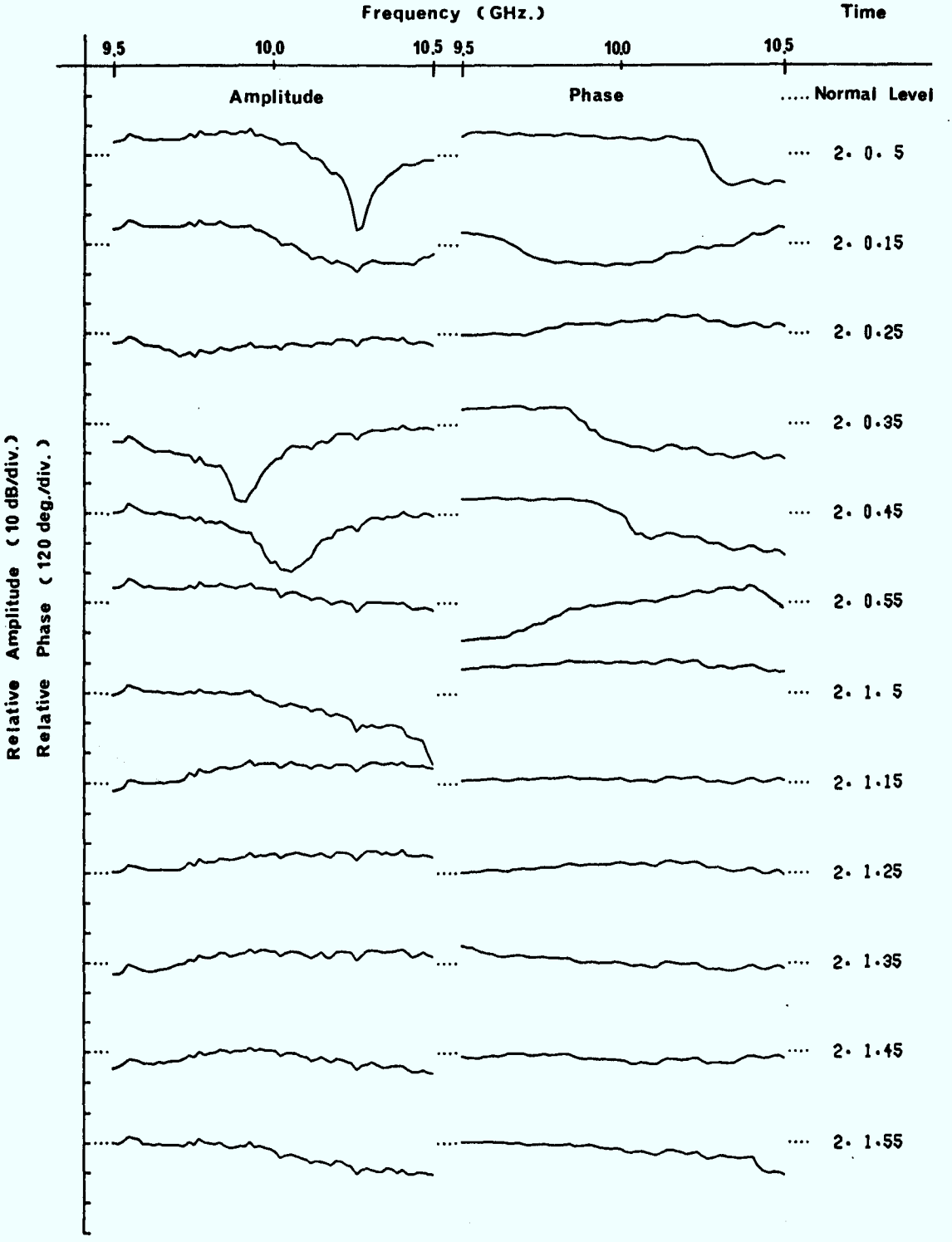

Fig. 3-15(c) Consecutive Sweep Records from Diagnostic System on 4th August (day 216) showing fast fading with short relative delay

moderate to severe fading activities) and should be useful as a worst case reference.

The experimental observations under quiet conditions were well explained by the path geometry, and most of the time two received rays with a relative delay of $\sim$ 4.5 nsec were observed. The terrain blockage offered by the North Mountain to the reflection from the sea was adequate down to dN/dh values of approximately -140 NU/Km, at least under conditions of uniform refractivity gradients. However, the same is not true under certain atmospheric conditions, as will be discussed later.

The angle-of-arrival variations observed over five days of quiet conditions resulted in a 99.9% range of $\sim$ 0.7 deg. With proper scaling to a one year period and accounting for seasonal variations, an estimate of over 1 deg for a 99.9% range over a year is not considered unreasonable. Communications antenna beamwidth requirements should be reviewed in the light of this result, especially when one considers the fact that most antennas are usually less than perfectly aligned.

Propagation conditions during active fading days (e.g. 29th and 30th August) are not as readily explained by the path geometry and a simple model of uniform refractivity gradient. Although a 9 nsec delay is possible with a uniform gradient of approximately -200 NU/Km, the ray path amplitudes and AOA's were incorrectly predicted. Since the phenomenon was only observed on a few days during the experiment, some

anomalous atmospheric effects are expected to be associated with such observations. One possible set of explanations involves the presence of an atmospheric layer or duct.

By employing a ray tracing technique (Webster, 1982) the effect of the presence of such an atmospheric duct is shown in Figures 4-1a to c for the same duct at different elevations. The defocussing effect of the duct on the direct ray shown in Figure 4-1b is particularly interesting and accounted for the decrease in amplitude of the main received ray. At the same time, the reflected ray, which was normally blocked, was 'lifted' by the presence of the duct and cleared the blockage at the North Mountain, thus accounting for the increased amplitude of the reflected ray. These results are summarized in Figure 4-2 in which N_o is the ground refractivity, dN/dh is the basic profile, and Δ N is the change in refractivity over the height range Δ h. The elevations of the transmit and receive antennas are also shown in the figure, and h_s, the height of the reflected ray at the North Mountain, was included to provide an idea of the clearance above the landscape which is indicated by N.M. in the figure. The reader should note in particular the defocussing effect of the duct on the direct ray labelled 1 and also the existence of atmospheric multipath in case of a high level layer. For a more comprehensive discussion of such atmospheric multipaths, the reader is referred to Webster (1982).

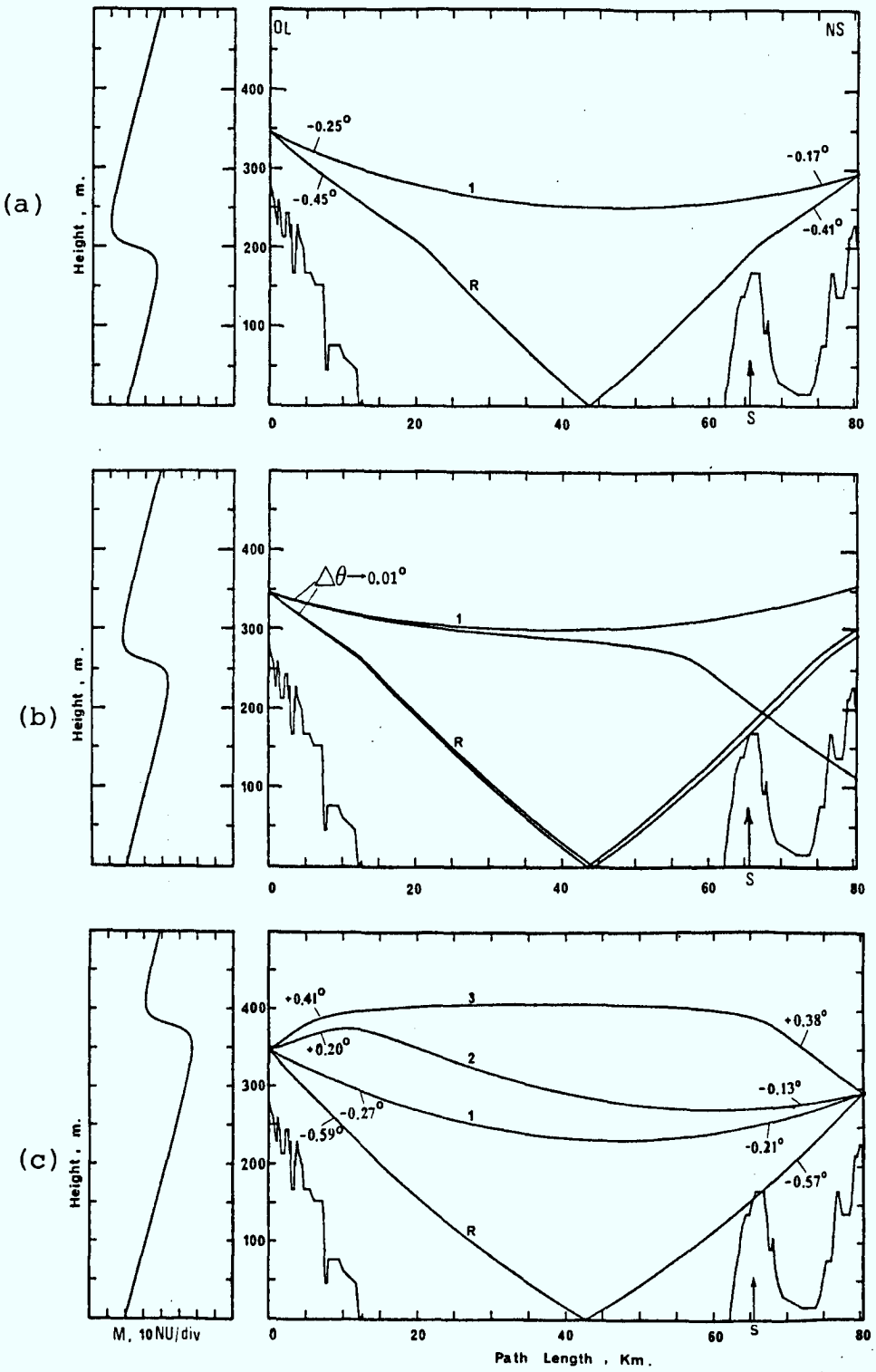

Fig. 4-1 Ray Tracing for Otter Lake - Nictaux South link when a layer is present at various elevations:
(a) Low-level layer
(b) Mid-level layer
(c) High-level layer

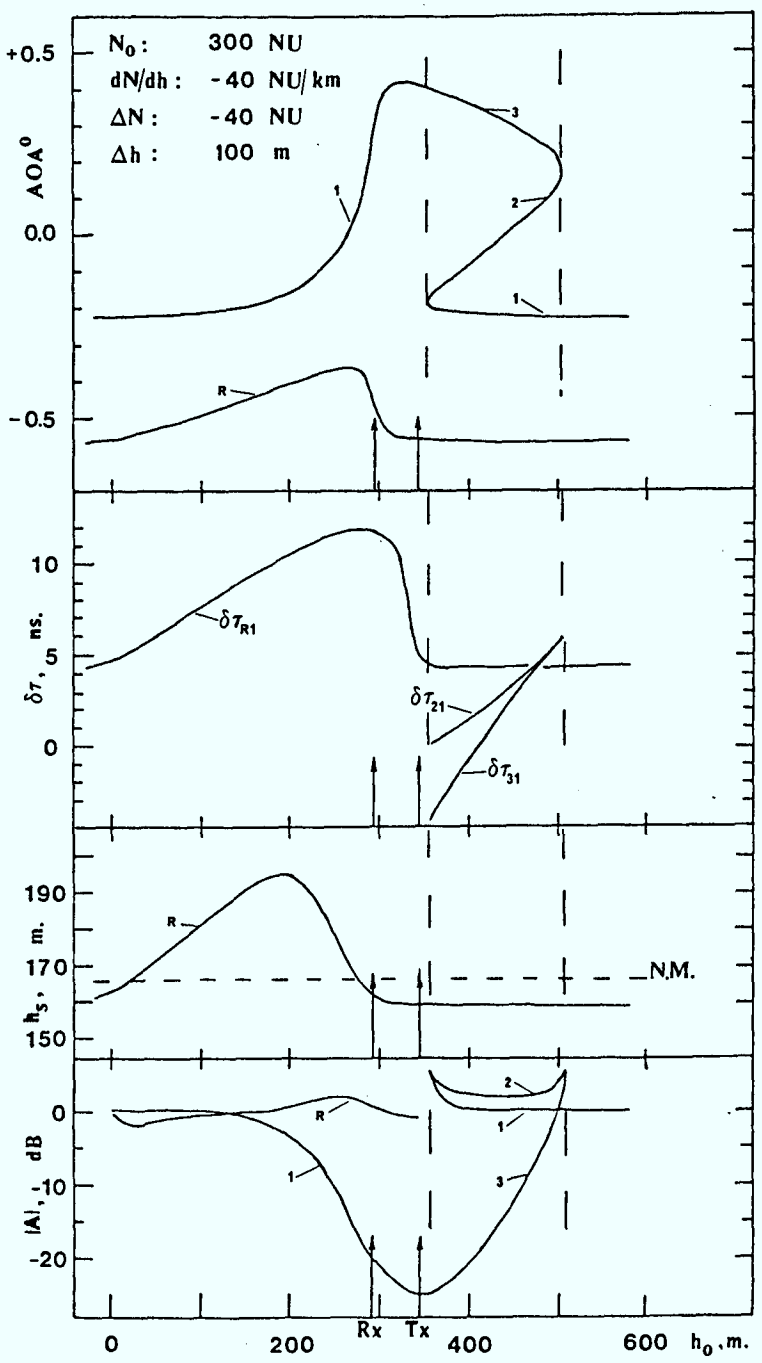

Fig. 4-2 Effects of layer height variations on the received ray path parameters - Otter Lake to Nictaux South link

As regards the performance of the digital radio, the results so far indicated a correlation between high BER's and a combination of long echo-delays (of up to 10 nsec) and low differential amplitudes in case of two received ray paths. As pointed out earlier, this is due to the higher probability of in-band nulls when long delay ray paths are present (recalling that the number of nulls in, say, a 1 GHz band doubles if the relative delay in nsec is doubled). As would be expected, the situation is worsened by a wide radio bandwidth. This last observation is also closely related to frequency diversity requirements and further analysis is expected to provide useful information on this and other topics related to propagation path designs.

ACKNOWLEDGEMENTS

The close cooperation of Maritime Tel. and Tel. and New Brunswick Tel. during the experiment is greatly appreciated. The authors would like to acknowledge the useful discussions with personnel at the C.R.C. and in the Centre for Radio Science. The authors would also like to thank Mr. M.P. Pothier for extra efforts beyond his normal duties at M.T. & T., Mrs. M. Meighen for help in the typing; and Mr. D.J. Chen for help in the preparation of the diagrams.

REFERENCES

Segal, B. and R.E. Barrington. Tropospheric Refractivity Atlas for Canada. C.R.C. Report No. 1315-E, 1977.

Webster, A.R., Forsyth, P.A. & T. Ueno. A Study for the Development and Testing of a Microwave Diagnostic System. C.R.C. Report, DSS Contract No. 01SU.36001-6-2317, 1977.

Webster, A.R. and W.I. Lam. Operation of an Experimental Microwave Link between Otter Lake, N.B. and Aylesford, N.S. C.R.C. Report, DSS Contract No. 18ST.36001-0-3173, 1981.

Webster, A.R. "Raypath Parameters in Tropospheric Multipath Propagation". IEEE Transactions on Antennas and Propagation, vol. AP-30, No. 4, July, 1982.

Webster, A.R. "Angles-of-Arrival and Delay Times on Terrestrial Line-of-Sight Microwave Links". To be published in IEEE Transactions on Antennas and Propagation, 1982.

White, R.F. Engineering Considerations for Microwave Communications Systems. Lenkurt Electric Co. Inc., June, 1970.

APPENDIX A

Diagnostic System Details

Transmitted power:	∿ 1 watt
Transmit antenna:	8 ft. diameter paraboloid
Receive antennas:	2 ft. diameter paraboloids vertically spaced 3 m
Frequency sweep:	9.505-10.513 GHz, 64 steps 16 MHz per step
Sweep time:	1.28 sec
Repetition period:	10 sec
Recording:	digital, 8 bits each, amplitude and phase

APPENDIX B

Propagation Path Parameters

Year	1980	1981
Path Length, Km	80.025	80.375
N.B. Site		
Location	Otter Lake	Otter Lake
Latitude	45°22'10"N	45°22'10"N
Longitude	65°46'23"W	65°46'23"W
Ground Elevation, m	279	279
Antenna Height, m	6	69
N.S. Site		
Location	Aylesford	Nictaux South
Latitude	45° 04'26"N	44° 52'00"N
Longitude	64° 50'30"W	65° 02'10"W
Ground Elevation, m	239	216
Antenna Height, m	14	81